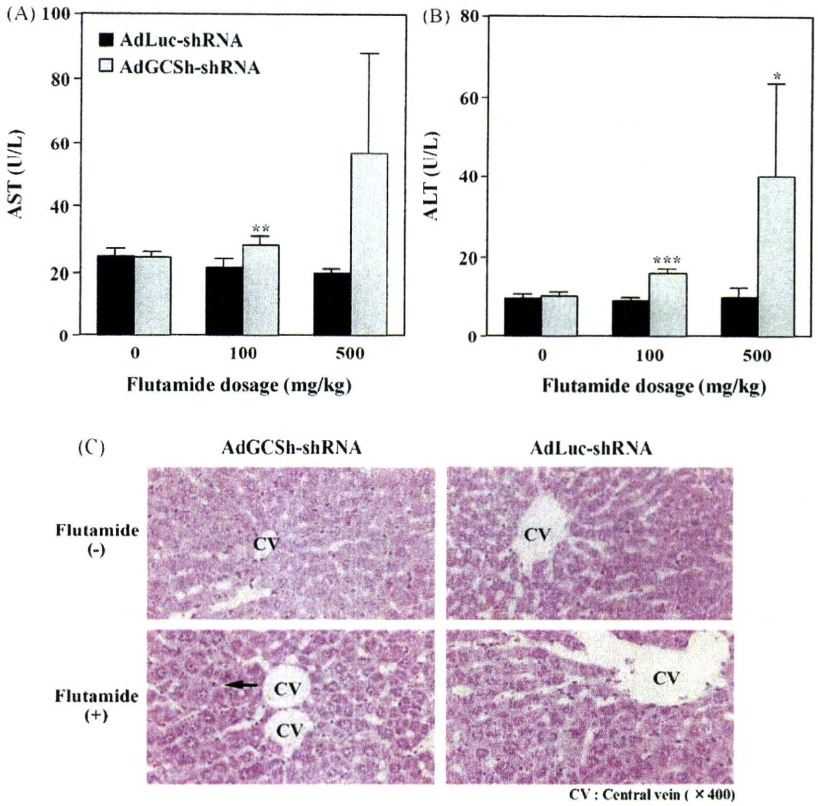

Fig. 3. Subacute hepatotoxic effect of flutamide in γ-GCS-knockdown rats. Flutamide was p.o. administered once a day for a week. Twenty-four hours after the last administration, serum AST (A) and ALT (B) were measured, and hematoxylin-eosin staining (C) was performed in sections of rat liver. Degenerated hepatocyte shown by arrowhead was observed only in flutamide-administered γ-GCS-knockdown rats. Data are mean ± SD ($n = 3–5$). $^*P < 0.05$, $^{**}P < 0.01$, and $^{***}P < 0.001$ compared with each AdLuc-shRNA-infected group.

rats administered with 100 mg/kg flutamide demonstrated a significant increase of AST and ALT, but the increases were small (Fig. 3A and B). Histological examination revealed degenerated and dropped-out hepatocytes in γ-GCS-knockdown rats given 500 mg/kg flutamide, consistent with the elevation of AST and ALT. There was no histological change in the other groups.

3.4. Confirmation of γ-GCS-knockdown in diclofenac- or flutamide-administered rats

Fourteen days after an intravenous injection of 1.5×10^{11} pfu/ml/body AdGCSh-shRNA, hepatic GSH was depleted by 80% (Akai et al., 2007). To determine whether such GSH depletion also occurred in the present study, the hepatic GSH level was measured (Fig. 4). Hepatic GSH was significantly decreased by AdGCSh-shRNA-infection compared with AdLuc-shRNA-infection. In addition, hepatic GSH was significantly increased by the administration of flutamide in AdLuc-shRNA-infected control rats compared with no drug administered group.

4. Discussion

We previously established the AdGCSh-short hairpin RNA (shRNA)-mediated GSH depletion rat model (Akai et al., 2007). This γ-GCS-knockdown rat model showed significantly potentiated drug-induced hepatotoxicity by the administration of acetaminophen (Akai et al., 2007). Diclofenac and flutamide are now widely used for medical treatment. However, occasionally, their hepatotoxicity in human has been reported. There is no appropriate animal model to evaluate diclofenac- and flutamide-induced hepatotoxicity. We hypothesized that GSH would be mainly involved in the hepatotoxicity of these drugs in rat, and the γ-GCS-knockdown rat model could demonstrate the hepatotoxic effects of these drugs.

In the diclofenac-induced 6 h hepatotoxicity study, only in 100 mg/kg diclofenac administered γ-GCS-knockdown rats was hepatotoxicity observed (Fig. 1). However, no typical histological change was observed. Gastrointestinal and cardiovascular events, not only hepatotoxicity, are major adverse events of diclofenac (Hippisley-Cox et al., 2005; Waksman et al., 2007). Thus, diclofenac was intraperitoneally administered in the present study to avoid gastrointestinal effects. In diclofenac administered rats, the AST and ALT levels were increased in the present study. The AST level is associated with hepatotoxicity, but also can be elevated in association with other diseases, for example, heart and skeletal muscle injury (Burhop et al., 2004; Lott and Landesman, 1984). In the present study, involvement of cardio- or muscle-toxicity can not be excluded. The AST and ALT increases were attenuated after 24 h, compared with those after 6 h. In the present study, we were not able to demonstrate subacute hepatotoxicity by 7 days study. There has been no report of subacute hepatotoxicity in a rat model, but the present study firstly demonstrated that the γ-GCS-knockdown rat is sensitive to diclofenac-induced acute hepatotoxicity by 6 and 24 h study.

Regarding diclofenac, two hypotheses of the mechanism by which hepatotoxicity develops have been proposed. The first implicates the reactive acylglucuronide of diclofenac as a potential causative agent (Pumford et al., 1993; Hargus et al., 1994). The second is based upon the observation of an NADPH-dependent covalent modification of proteins by incubation of the drug with

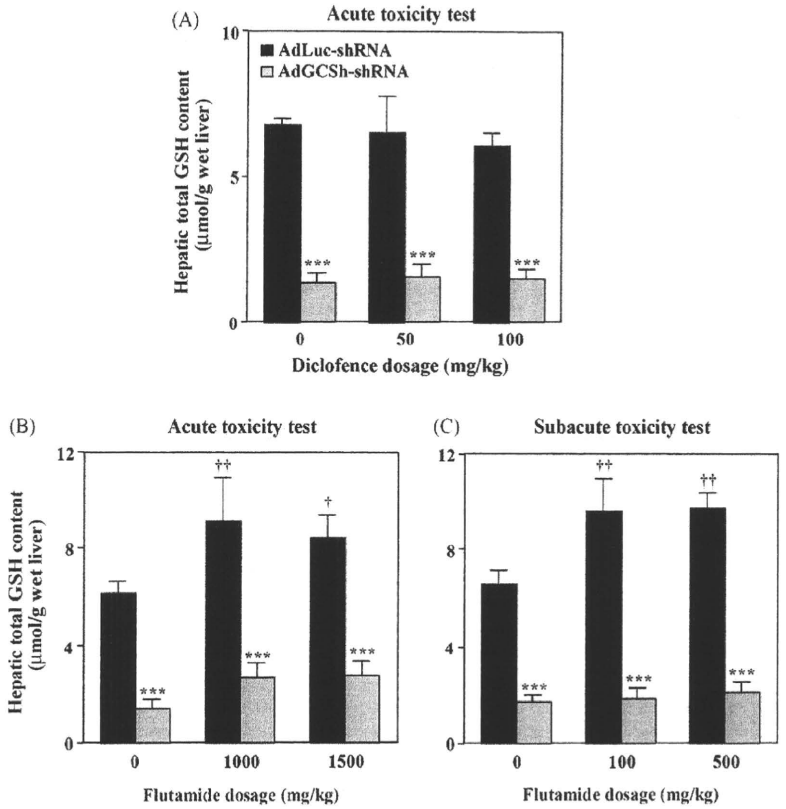

Fig. 4. Total GSH content in diclofenac or flutamide administered γ-GCS-knockdown rats. Total hepatic GSH content was measured 6 h after the administration in the acute toxicity test of diclofenac (A), 24 h after administration in the acute toxicity test of flutamide (B) and 24 h after the last administration in the subacute toxicity test of flutamide (C). Data are mean ± SD ($n = 3–5$). ***$P < 0.001$ compared with each AdLuc-shRNA-infected group (Student's t-test). †$P < 0.05$ and ††$P < 0.01$ compared with AdLuc-shRNA-infected and no drug administered group (Dunnett's post hoc test).

rat or human microsomes and the formation of GSH or mercapturic acid conjugates in rats treated with the drug (Tang et al., 1999; Poon et al., 2001). In the present study, supporting the latter hypothesis, the involvement of GSH in the diclofenac-induced acute hepatotoxicity was demonstrated. However, it is unclear that the involvement of acylglucuronide in diclofenac-induced hepatotoxicity in the present study.

In the flutamide-induced 24 h hepatotoxicity study, the γ-GCS-knockdown rats showed similar hepatotoxicity when administered 1000 and 1500 mg/kg (Fig. 2). This could be caused by saturated absorption. We also investigated of 500 mg/kg flutamide in 24 h study, and no hepatotoxicity was observed (data not shown). In addition, the bilirubin level was slightly increased in γ-GCS-knockdown rats administered flutamide at 1000 and 1500 mg/kg, however, cholestasis was not observed by histology. This is the first report of flutamide-induced acute hepatotoxicity in rat.

Flutamide-induced subacute hepatotoxicity (100 mg/kg for 15 days) was reported by Mannaa et al. (2005). In our study, rats were administered flutamide at 100 or 500 mg/kg for 7 days and ALT was significantly elevated. Histological hepatotoxicity was also observed. This condition is different from that described by Mannaa et al. (2005). Nevertheless, the γ-GCS-knockdown rat is the first successful model sensitive for flutamide-induced acute and subacute hepatotoxicity.

Although the mechanisms of flutamide-induced hepatotoxicity have not been precisely elucidated, CYP-mediated oxidative bioactivation to reactive metabolites is thought to be a cause of the toxicity (Berson et al., 1993; Fau et al., 1994). Recently, GSH or mercapturic acid conjugates of flutamide were detected in human liver microsomes or urine of prostate cancer patients (Kang et al., 2007; Soglia et al., 2006; Tevell et al., 2006). Conjugates of flutamide were also detected in mouse liver microsomes (Ohbuchi et al., 2009). In the present study, the involvement of GSH in the flutamide-induced acute and subacute hepatotoxicity was clearly demonstrated. In addition, GSH depleted mice showed hepatotoxicity (ALT; 200 IU/L) when administered 400 mg/kg of flutamide (Matsuzaki et al., 2006). GSH content was reduced to 27% of normal mice with an amino acid-deficient diet for 2 weeks. This hepatotoxicity was not observed without amino acid-deficient diet (Matsuzaki et al., 2006). These data supported the involvement of GSH in the flutamide-induced hepatotoxicity.

Diclofenac- or flutamide-induced subacute hepatotoxicity was not detected or lower than acute hepatotoxicity in the present rat model. Responsiveness to toxicity of a drug occasionally decreases resulting from prior exposure to that drug, which is generically called tolerance. The major mechanisms for tolerance are as follows, one is due to decreased amount toxicant reaching the site where the toxicity is produced. The other is due to reduced responsiveness of a tissue to the drug (Eaton and Klaassen, 2001). In the present study, subacute hepatotoxicity would be lowered by tolerance, however the mechanism is awaited to be clarified.

Hepatic GSH content was successfully knockdown by AdGCSh-shRNA in diclofenac administered groups. On the other hand, hepatic GSH was increased by the administration of flutamide (Fig. 4). Hepatic γ-GCS is regulated by nuclear factor-erythroid 2-related factor 2 (Nrf2) (Copple et al., 2008). Nrf2 is partly regulated by protein kinase C (PKC) (Huang et al., 2002; Numazawa et al., 2003) and flutamide increases PKC expression (Montalvo

et al., 2002). Thus, flutamide could increase oxidative stress and PKC expression, and then hepatic GSH could be increased due to the induction of γ-GCS. In 7 days flutamide hepatotoxicity study, hepatic GSH content was induced in the control rats, but not in the γ-GCS knockdown rats, demonstrating the continuous knockdown of γ-GCS. However, GSH would be used to detoxify flutamide, and intrahepatic level should be decrease instead of increase. Further investigation would be needed to clarify this mechanism.

The maximum depletion of GSH was obtained 14 days after AdGCSh-shRNA infection in rats and continued about 2 weeks (Akai et al., 2007). Therefore, to maintain the GSH depletion level, we conducted the subacute toxicity study for a short time (7 days). In particular, we started drug administration 10 days after the injection and continued for a week. This would be enough time to determine the onset of hepatotoxicity.

The activity of hepatic glutathione *S*-transferase (GST) and hepatic GSH content is 10–20 times and about 2 times higher in rodent than that of humans, respectively (Grover and Sims, 1964; Woodhouse et al., 1983; Higashi et al., 1985). GSH conjugation plays an important role in protecting tissues, it is hard to predict DILI in preclinical study using rat. In addition, although *in vitro* test to detect reactive intermediates by GSH adduct is widely used, these data could not always correlate with *in vivo* (Soglia et al., 2006; Evans et al., 2004). It is partly because some GSH adducts are not stable and are subject to chemical degradation/rearrangement or enzymatic degradation, thereby escaping detection (Evans et al., 2004). In the present study, we could show the γ-GCS-knockdown rat model sensitively detect diclofenac- and flutamide-induced hepatotoxicity. Thus, decreasing glutathione levels in a rat model would be relevant and predictive of DILI in humans.

The present rat model is sensitive for hepatotoxic drugs compared to the normal rat. However, it is difficult to determine the absolute dosage of drugs for the purpose of extrapolating the hepatotoxicity in human. The present rat model has an advantage to compare the hepatotoxicity in structurally related compounds in drug development process.

In summary, in the present study, we demonstrated that the γ-GCS-knockdown rat model can sensitively detect diclofenac- and flutamide-induced hepatotoxicity, indicating the involvement of GSH in the hepatotoxic effect of these drugs. Thus, this rat model could be useful for highly sensitive tests to evaluating acute and subacute DILI in preclinical drug development.

Conflict of interest statement

The authors declare that there are no conflicts of interest.

Acknowledgements

We thank Mr. Brent Bell for reviewing the manuscript. This work was supported by Health and Labor Science research grants from the Ministry of Health, Labor and Welfare of Japan.

References

Aithal, G.P., Day, C.P., 2007. Nonsteroidal anti-inflammatory drug-induced hepatotoxicity. Clin. Liver Dis. 11, 563–575.

Akai, S., Hosomi, H., Minami, K., Tsuneyama, K., Katoh, M., Nakajima, M., Yokoi, T., 2007. Knock down of γ-glutamylcysteine synthetase in rat causes acetaminophen-induced hepatotoxicity. J. Biol. Chem. 282, 23996–24003.

Berson, A., Wolf, C., Chachaty, C., Fisch, C., Fau, D., Eugene, D., Loeper, J., Gauthier, J.C., Beaune, P., Pompon, D., Maurel, P., Pessayre, D., 1993. Metabolic activation of the nitroaromatic antiandrogen flutamide by rat and human cytochromes P-450, including forms belonging to the 3A and 1A subfamilies. J. Pharmacol. Exp. Ther. 265, 366–372.

Burhop, K., Gordon, D., Estep, T., 2004. Review of hemoglobin-induced myocardial lesions. Artif. Cells Blood Substit. Immobil. Biotechnol. 32, 353–374.

Copple, I.M., Goldring, C.E., Kitteringham, N.R., Park, B.K., 2008. The Nrf2-Keap1 defence pathway: role in protection against drug-induced toxicity. Toxicology 246, 24– 33.

Dalton, T.P., Dieter, M.Z., Yang, Y., Shertzer, H.G., Nebert, D.W., 2000. Knockout of the mouse glutamate cysteine ligase catalytic subunit (Gclc) gene: embryonic lethal when homozygous, and proposed model for moderate glutathione deficiency when heterozygous. Biochem. Biophys. Res. Commun. 279, 324–329.

Davies, N.M., Anderson, K.E., 1997. Clinical pharmacokinetics of diclofenac: therapeutic insights and pitfalls. Clin. Pharmacokinet. 33, 184–213.

Eaton, D.L., Klaassen, C.D., 2001. Principles of toxicology. In: Klaassen, C.D. (Ed.), Casarett and Doull's Toxicology: The Basic Science of Poisons, sixth ed. McGraw-Hill, NY, pp. 11–34.

Evans, D.C., Watt, A.P., Nicoll-Griffith, D.A., Baillie, T.A., 2004. Drug-protein adducts: an industry perspective on minimizing the potential for drug bioactivation in drug discovery and development. Chem. Res. Toxicol. 17, 3–16.

Fau, D., Eugene, D., Berson, A., Letteron, P., Fromenty, B., Fisch, C., Pessayre, D., 1994. Toxicity of the antiandrogen flutamide in isolated rat hepatocytes. J. Pharmacol. Exp. Ther. 269, 954–962.

Gad, S.C., 2007. The mouse, toxicology. In: Gad, S.C. (Ed.), Animal models in Toxicology, second ed. Applied Taylor & Francis, Boca Raton, pp. 24–72.

García-Cortés, M., Andrade, R.J., Lucena, M.I., Sánchez-Martínez, H., Fernández, M.C., Ferrer, T., Martín-Vivaldi, R., Peláez, G., Suárez, F., Romero-Gómez, M., Montero, J.L., Fraga, E., Camargo, R., Alcántara, R., Pizarro, M.A., García-Ruiz, E., Rosemary-Gómez, M., 2001. Flutamide-induced hepatotoxicity: report of a case series. Rev. Esp. Enferm. Dig. 93, 423–432.

Grover, P.L., Sims, P., 1964. Conjugations with glutathione. Distribution of glutathione S-aryltransferase in vertebrate species. Biochem. J. 90, 603–606.

Hargus, S.J., Amouzedeh, H.R., Pumford, N.R., Myers, T.G., McCoy, S.C., Pohl, L.R., 1994. Metabolic activation and immunochemical localization of liver protein adducts of the nonsteroidal anti-inflammatory drug diclofenac. Chem. Res. Toxicol. 7, 575– 582.

Higashi, T., Furukawa, M., Hikita, K., Naruse, A., Tateishi, N., Sakamoto, Y., 1985. Re-evaluation of protein-bound glutathione in rat liver. J. Biochem. 98, 1661–1667.

Hippisley-Cox, J., Coupland, C., Logan, R., 2005. Risk of adverse gastrointestinal outcomes in patients taking cyclooxygenase-2 inhibitors or conventional non-steroidal anti-inflammatory drugs: population based nested case-control analysis. Br. Med. J. 331, 1310–1316.

Huang, C.S., Anderson, M.E., Meister, A., 1993a. Amino acid sequence and function of the light subunit of rat kidney γ-glutamylcysteine synthetase. J. Biol. Chem. 268, 20578–20583.

Huang, C.S., Chang, L.S., Anderson, M.E., Meister, A., 1993b. Catalytic and regulatory properties of the heavy subunit of rat kidney γ-glutamylcysteine synthetase. J. Biol. Chem. 268, 19675–19680.

Huang, H.C., Nguyen, T., Pickett, C.B., 2002. Phosphorylation of Nrf2 at Ser-40 by protein kinase C regulates antioxidant response element-mediated transcription. J. Biol. Chem. 277, 42769–42774.

Johnson, M.D., 2007. The rat, toxicology. In: Gad, S.C. (Ed.), Animal models in Toxicology, second ed. Applied Taylor & Francis, Boca Raton, pp. 150–193.

Kang, P., Dalvie, D., Smith, E., Zhou, S., Deese, A., 2007. Identification of a novel glutathione conjugate of flutamide in incubations with human liver microsomes. Drug Metab. Dispos. 35, 1081–1088.

Kaplowitz, N., 2005. Idiosyncratic drug hepatotoxicity. Nat. Rev. Drug Discov. 4, 489–499.

Lott, J.A., Landesman, P.W., 1984. The enzymology of skeletal muscle disorders. Crit. Rev. Clin. Lab. Sci. 20, 153–190.

Makarova, S.I., 2008. Human N-acetyltransferases and drug-induced hepatotoxicity. Curr. Drug Metab. 9, 538–545.

Mannaa, F., Ahmed, H.H., Estefan, S.F., Sharaf, H.A., Eskander, E.F., 2005. Saccharomyces cerevisiae intervention for relieving flutamide-induced hepatotoxicity in male rats. Pharmazie 60, 689–695.

Matsuzaki, Y., Nagai, D., Ichimura, E., Goda, R., Tomura, A., Doi, M., Nishikawa, K., 2006. Metabolism and hepatic toxicity of flutamide in cytochrome P450 1A2 knockout SV129 mice. J. Gastroenterol. 41, 231– 239.

Meister, A., Anderson, M.E., 1983. Glutathione. Annu. Rev. Biochem. 52, 711–760.

Montalvo, L., Sánchez-Chapado, M., Prieto, J.C., Carmena, M.J., 2002. Regulation of the expression of protein kinase C isoenzymes in rat ventral prostate: effects of age, castration and flutamide treatment. Life Sci. 71, 2257–2266.

Numazawa, S., Ishikawa, M., Yoshida, A., Tanaka, S., Yoshida, T., 2003. Atypical protein kinase C mediates activation of NF-E2-related factor 2 in response to oxidative stress. Am. J. Physiol. Cell Physiol. 285, C334–C342.

Ohbuchi, M., Miyata, M., Nagai, D., Shimada, M., Yoshinari, K., Yamazoe, Y., 2009. Role of enzymatic N-hydroxylation and reduction in flutamide metabolite-induced liver toxicity. Drug Metab. Dispos. 37, 97– 105.

Poon, G.K., Chen, Q., Teffera, Y., Ngui, J.S., Griffin, P.R., Braun, M.P., Doss, G.A., Freeden, C., Stearns, R.A., Evans, D.C., Baillie, T.A., Tang, W., 2001. Bioactivation of diclofenac via benzoquinone imine intermediates-identification of urinary mercapturic acid derivatives in rats and humans. Drug Metab. Dispos. 29, 1608–1613.

Pumford, N.R., Myers, T.G., Davila, J.C., Highet, R.J., Pohl, L.R., 1993. Immunochemical detection of liver protein adducts of the nonsteroidal antiinflammatory drug diclofenac. Chem. Res. Toxicol. 6, 147–150.

Reed, D.J., 1986. Regulation of reductive processes by glutathione. Biochem. Pharmacol. 35, 7–13.

Soglia, J.R., Contillo, L.G., Kalgutkar, A.S., Zhao, S., Hop, C.E., Boyd, J.G., Cole, M.J., 2006. A semiquantitative method for the determination of reactive metabolite conjugate levels in vitro utilizing liquid chromatography-tandem mass spectrometry

and novel quaternary ammonium glutathione analogues. Chem. Res. Toxicol. 19, 480–490.
Tang, W., Stearns, R.A., Bandiera, S.M., Zhang, Y., Raab, C., Braun, M.P., Dean, D.C., Pang, J., Leung, K.H., Doss, G.A., Strauss, J.R., Kwei, G.Y., Rushmore, T.H., Chiu, S.H., Baillie, T.A., 1999. Studies on cytochrome P-450-mediated bioactivation of diclofenac in rats and in human hepatocytes: identification of glutathione conjugated metabolites. Drug Metab. Dispos. 27, 365–372.
Tevell, A., Lennernäs, H., Jönsson, M., Norlin, M., Lennernäs, B., Bondesson, U., Hedeland, M., 2006. Flutamide metabolism in four different species in vitro and identification of flutamide metabolites in human patient urine by high performance liquid chromatography/tandem mass spectrometry. Drug Metab. Dispos. 34, 984–992.
Tietze, F., 1969. Enzymatic method for quantitative determination of nanogram amounts of total and oxidized glutathione: applications to mammalian blood and other tissues. Anal. Biochem. 27, 502–522.
Waksman, J.C., Brody, A., Phillips, S.D., 2007. Nonselective nonsteroidal antiinflammatory drugs and cardiovascular risk: are they safe? Ann Pharmacother. 41, 1163–11173.
Woodhouse, K.W., Williams, F.M., Mutch, E., Wright, P., James, O.F., Rawlins, M.D., 1983. The effect of alcoholic cirrhosis on the activities of microsomal aldrin epoxidase, 7-ethoxycoumarin O-de-ethylase and epoxide hydrolase, and on the concentrations of reduced glutathione in human liver. Br. J. Clin. Pharmacol. 15, 667–672.

0090-9556/09/3707-1513–1520$20.00
DRUG METABOLISM AND DISPOSITION

DMD 37:1513–1520, 2009

Vol. 37, No. 7
26567/3478493
Printed in U.S.A.

Human Arylacetamide Deacetylase Is a Principal Enzyme in Flutamide Hydrolysis

Akinobu Watanabe, Tatsuki Fukami, Miki Nakajima, Masataka Takamiya, Yasuhiro Aoki, and Tsuyoshi Yokoi

Drug Metabolism and Toxicology, Faculty of Pharmaceutical Sciences, Kanazawa University, Kakuma-machi, Kanazawa, Japan (A.W., T.F., M.N., T.Y.); and Department of Legal Medicine, Iwate Medical University School of Medicine, Uchimaru, Morioka, Japan (M.T., Y.A.)

Received January 19, 2009; accepted March 26, 2009

ABSTRACT:

Flutamide, an antiandrogen drug, is widely used for the treatment of prostate cancer. The initial metabolic pathways of flutamide are hydroxylation and hydrolysis. It was recently reported that the hydrolyzed product, 4-nitro-3-(trifluoromethyl)phenylamine (FLU-1), is further metabolized to *N*-hydroxy FLU-1, an assumed hepatotoxicant. However, the esterase responsible for the flutamide hydrolysis has not been characterized. In the present study, we found that human arylacetamide deacetylase (AADAC) efficiently hydrolyzed flutamide using recombinant AADAC expressed in COS7 cells. In contrast, carboxylesterase1 (CES1) and CES2, which are responsible for the hydrolysis of many drugs, could not hydrolyze flutamide. AADAC is specifically expressed in the endoplasmic reticulum. Flutamide hydrolase activity was highly detected in human liver microsomes (K_m, 794 ± 83 μM; V_{max}, 1.1 ± 0.0 nmol/min/mg protein), whereas the activity was extremely low in human liver cytosol. The flutamide hydrolase activity in human liver microsomes was strongly inhibited by bis-(nonylphenyl)-phenylphosphate, diisopropylphosphorofluoride, and physostigmine sulfate (eserine) but moderately inhibited by sodium fluoride, phenylmethylsulfonyl fluoride, and disulfiram. The same inhibition pattern was obtained with the recombinant AADAC. Moreover, human liver and jejunum microsomes showing AADAC expression could hydrolyze flutamide, but human pulmonary and renal microsomes, which do not express AADAC, showed slight activity. In human liver microsomal samples (n = 50), the flutamide hydrolase activities were significantly correlated with the expression levels of AADAC protein (r = 0.66, p < 0.001). In conclusion, these results clearly showed that flutamide is exclusively hydrolyzed by AADAC. AADAC would be an important enzyme responsible for flutamide-induced hepatotoxicity.

Flutamide (3′-trifluoro-2-methyl-4′-nitro-2-methyl-propinoylanilide) is a nonsteroidal antiandrogen drug used for the treatment of prostate cancer. The combination of luteinizing hormone-releasing hormone agonist results in prolonged survival in prostate cancer patients (Crawford et al., 1989). However, flutamide occasionally causes severe hepatotoxicity (Thole et al., 2004). Flutamide itself is not toxic when used at the appropriate clinical dose, but bioactivation of flutamide has been considered to be the cause of flutamide-induced hepatotoxicity (Fau et al., 1994).

Flutamide is mainly metabolized to 2-hydroxyflutamide by human CYP1A2. It has been suggested that 2-hydroxyflutamide is associated with the therapeutic effect of flutamide (Katchen and Buxbaum, 1975). Flutamide is also hydrolyzed to 4-nitro-3-(trifluoromethyl)phenylamine (FLU-1) by esterase (Katchen and Buxbaum, 1975; Schulz et al., 1988). FLU-1 is considered to have no therapeutic effect (Aizawa et al., 2003). Goda et al. (2006) recently reported that FLU-1 is further metabolized to *N*-hydroxyl FLU-1 by human CYP3A4. Many researchers have reported on the relationship between the toxicity and metabolism of flutamide. It was shown in CYP1A2 knockout SV129 mice but not in wild-type mice that the urinary concentration of FLU-1 was increased, and an abnormal elevation of alanine aminotransferase was shown after the knockout mice were fed an amino acid-deficient diet (Matsuzaki et al., 2006). It was also shown in humans that the urinary caffeine metabolite ratio, an indicator of the CYP1A2 activity, was significantly lower in patients with hepatic injury compared with patients with normal hepatic function after the same flutamide therapy (Ozono et al., 2002). In addition, a study on patients of prostate cancer taking flutamide showed that the incidence of hepatotoxicity was correlated with the plasma concentration of FLU-1 (Aizawa et al., 2003). More recently, Ohbuchi et al. (2009) reported that coadministration of FLU-1 and 1,4-bis[2-(3,5-dichloropyridyloxy)]benzene, an inducer of CYP3A and CYP1A, to mice significantly increased serum alanine aminotransferase, and sev-

Article, publication date, and citation information can be found at http://dmd.aspetjournals.org.
doi:10.1124/dmd.109.026567.

ABBREVIATIONS: FLU-1, 4-nitro-3-(trifluoromethyl)phenylamine; CES, carboxylesterase; HLM, human liver microsome; BNPP, bis-(nonylphenyl)-phenylphosphate; AADAC, arylacetamide deacetylase; DFP, diisopropylphosphorofluoride; eserine, physostigmine sulfate; PMSF, phenylmethylsulfonyl fluoride; $AgNO_3$, silver nitrate; $CdCl_2$, cadmium chloride; $CoCl_2$, cobaltous chloride; $CuCl_2$, cupric chloride; PNPA, *p*-nitrophenyl acetate; NaF, sodium fluoride; HLC, human liver cytosol; HJM, human jejunum microsome; HPM, human pulmonary microsome; HRM, human renal microsome; RT-PCR, reverse transcription-polymerase chain reaction; GAPDH, glyceraldehyde 3-phosphate dehydrogenase; SNP, single nucleotide polymorphism; DMSO, dimethyl sulfoxide; HPLC, high-performance liquid chromatography.

eral protein adducts were detected after incubation of the microsomal protein with *N*-hydroxy FLU-1. Therefore, the hepatotoxicity of flutamide might be related to *N*-hydroxy FLU-1. Considering these reports, the hydrolysis pathway may contribute to the hepatotoxicity of flutamide.

Carboxylesterase (CES) is the major serine esterase contributing to the hydrolysis of various drugs and xenobiotics. In human, CES isoforms are classified into three families: CES1, CES2, and CES3. CES1 and CES2 have been reported to be responsible for the biotransformation of a number of clinically used drugs and prodrugs such as imidapril, capecitabine, and irinotecan (Imai et al., 2006). CES3 appears to show extremely low activity compared with CES1 and CES2 (Sanghani et al., 2004). The flutamide hydrolysis by human liver microsomes (HLM) is inhibited by bis-(nonylphenyl)-phenylphosphate (BNPP), a general CES inhibitor (Heymann and Krisch, 1967; Block and Arndt, 1978; Mentlein et al., 1988). Thus, it is plausible that flutamide is hydrolyzed by CES. However, the flutamide hydrolase activity was not detected by using purified CES1 (pI 4.5) and CES2 (pI 5.3) (Takai et al., 1997). Therefore, we considered that another esterase expressed in HLM plays a role in flutamide hydrolysis. As a candidate enzyme, arylacetamide deacetylase (AADAC) could be considered.

AADAC, as well as CES1 and CES2, is a major serine hydrolase expressed in HLM (Ross and Crow, 2007). AADAC was first identified as the enzyme that catalyzes the deacetylation of 2-acetylaminofluorene (Probst et al., 1991). The active site domain of AADAC shares high homology with that of hormone-sensitive lipase (Probst et al., 1994). Therefore, AADAC has been classified as a lipase. In fact, Tiwari et al. (2007) proved that human AADAC was capable of hydrolyzing cholesterol ester when expressed in yeast. However, it is unknown whether AADAC is involved in the hydrolysis of clinical therapeutic drugs. In the present study, the involvement of human AADAC in flutamide hydrolysis was investigated.

Materials and Methods

Chemicals and Reagents. Flutamide, 4-nitro-3-(trifluoromethyl)phenylamine (FLU-1), *p*-nitrophenol, diisopropylphosphorofluoride (DFP), physostigmine sulfate (eserine), phenylmethylsulfonyl fluoride (PMSF), disulfiram, silver nitrate ($AgNO_3$), cadmium chloride ($CdCl_2$), cobaltous chloride ($CoCl_2$), and cupric chloride ($CuCl_2$) were purchased from Wako Pure Chemical Industries (Osaka, Japan). *p*-Nitrophenyl acetate (PNPA), BNPP, and sodium fluoride (NaF) were purchased from Sigma-Aldrich (St. Louis, MO). Primers were commercially synthesized at Hokkaido System Sciences (Sapporo, Japan). The random hexamer and SYBR Premix Ex Taq were from Takara (Shiga, Japan). RevaTra Ace (Moloney murine leukemia virus reverse transcriptase RNase H−) was obtained from Toyobo (Tokyo, Japan). All the other chemicals used in this study were of analytical or the highest quality commercially available.

Human Tissues. The microsomes or cytosol from human liver, jejunum, lung, and kidney were used in this study. Pooled HLM (n = 50), individual HLM (24 donors), and pooled human liver cytosol (HLC, n = 22) were purchased from BD Gentest (Woburn, MA). Individual HLM from 15 donors were also obtained from Human and Animal Bridging Research Organization (Chiba, Japan), and those from 11 donors were obtained from autopsy materials that were discarded after pathological investigation. Human jejunum microsomes (HJM, pooled, n = 10), human pulmonary microsomes (HPM, single donor), and human renal microsomes (HRM, single donor) were purchased from Tissue Transformation Technologies (Edison, NJ). The pooled HLM, HJM, HPM, and HRM were used for the immunoblotting analysis and the assay of flutamide hydrolase activity. The HLC was used for the comparison of flutamide hydrolase activity with HLM. The individual HLM samples were used for the correlation analysis. The use of the human tissues was approved by the Ethics Committees of Kanazawa University (Kanazawa, Japan) and Iwate Medical University (Morioka, Japan).

TABLE 1

Primers used in the present study

Primer	Sequence
For detection of real-time RT-PCR	
AADAC-RT-S	5′-TTGTGGAGCTCCTGGGACTT-3′
AADAC-RT-AS	5′-TCTGTCTGCTGTCCATCTTG-3′
For construction of expression plasmids	
AADAC-S	5′-TAGAGACCAAGAAGCGGGAC-3′
AADAC-AS	5′-GCTACATGTTTTACTATAGATTTTCC-3′
CES1A1-S	5′-AGAGACCTCGCAGGCCCCGA-3′
CES1A2-S	5′-GAGACCTCGCAGGCCCCCG-3′
CES1A-AS	5′-CCATGGTAAGATGCCTTCTG-3′
CES2A1-S	5′-CCTGCCTACCACTAGATCCC-3′
CES2A1-AS	5′-CTCGCCTGTCAGCGAACCCAC-3′

Total RNA from Human Tissues and Reverse Transcription-Polymerase Chain Reaction Analyses. Total RNA samples from normal human liver (single donor), colon (pooled, n = 2), kidney (single donor), bladder (pooled, n = 2), breast (pooled, n = 2), ovary (single donor), and uterus (pooled, n = 3) were obtained from Stratagene (La Jolla, CA). Total RNA samples from normal human lung (single donor) and testis (single donor) were from Cell Applications (San Diego, CA). Total RNA samples from normal human stomach (single donor), adrenal gland (pooled, n = 62), and small intestine (pooled, n = 5) were from Clontech (Palo Alto, CA). The reverse transcription procedure was described previously (Nakajima et al., 2006).

For quantitative analysis, real-time reverse transcription-polymerase chain reaction (RT-PCR) was performed for AADAC mRNA using an MX3000P real-time PCR system (Stratagene). The forward and reverse primers used for PCR were AADAC-RT-S and AADAC-RT-AS primers (Table 1). A 1-μl portion of the reverse-transcribed mixture was added to a PCR mixture containing 10 pmol of each primer and 12.5 μl of SYBR Premix Ex Taq solution in a final volume of 25 μl. After an initial denaturation at 95°C for 30 s, the amplification was performed by denaturation at 94°C for 4 s, annealing at 58°C for 7 s, and extension at 72°C for 20 s for 45 cycles. Human glyceraldehyde 3-phosphate dehydrogenase (GAPDH) mRNA was also quantified according to a method described previously (Tsuchiya et al., 2004). The copy numbers were calculated using standard amplification curves.

Construction of Plasmids Expressing Human AADAC, CES1A, and CES2. The full-length human AADAC, CES1A1, CES1A2, and CES2A1 cDNAs were obtained by RT-PCR using a human liver RNA sample as the initial template. The primers used are shown in Table 1. In this study, two clones of AADAC cDNA were obtained [c.931guanine (G) and adenine (A)]. In the reference sequence of NM 001086.2, the nucleotide at the c.931 position is G. Therefore, the clones with c.931G and c.931A were defined as the AADAC wild-type and AADAC variant, respectively. This single nucleotide polymorphism (SNP, c.931G>A) leads to an amino acid change of valine to isoleucine. The allele frequency of this SNP (ID: rs1803155) has been reported to be approximately 55 to 80% in each population, including European, Asian, and sub-Saharan African in the dbSNP database in the National Center for Biotechnology Information (http://www.ncbi.nlm.nih.gov/SNP/snp_ref.cgi?rs = 1803155). The PCR products were subcloned into pTARGET mammalian expression vector (Promega, Madison, WI). The nucleotide sequences were confirmed by DNA sequence analysis (Long-Read Tower DNA sequencer; GE Healthcare, Little Chalfont, Buckinghamshire, UK).

Transfection of Plasmids Expressing Human AADAC, CES1A, and CES2. African green monkey kidney cells, COS7 cells, were obtained from American Type Culture Collection (Manassas, VA). The COS7 cells were grown in Dulbecco's modified Eagle's medium containing 4.5 g/l glucose and 10% fetal bovine serum with 5% CO_2 at 37°C. The cells were transfected in 10-cm dishes with 7.5 μg of each expression plasmid using Lipofectamine (Invitrogen, Carlsbad, CA). After incubation for 48 h, the cells were harvested and suspended in a small amount of TGE buffer (10 mM Tris-HCl, 20% glycerol, 1 mM EDTA, pH 7.4) and disrupted by freeze-thawing three times. Each protein expression level was determined by immunoblot analysis as described below.

Immunoblot Analysis. SDS-polyacrylamide gel electrophoresis and immunoblot analysis were performed according to Laemmli (1970). Enzyme sources (30 μg) were separated on 10% polyacrylamide gels and electrotransferred onto polyvinylidene difluoride membrane, Immobilon-P (Millipore Corporation, Billerica, MA). The membranes were probed with monoclonal mouse anti-human AADAC (Abnova, Neihu District, Taipei City, Taiwan), polyclonal rabbit anti-human CES1 (Abcam, Cambridge, MA), and polyclonal rabbit anti-human CES2 antibodies (Antagene, San Francisco, CA), and the corresponding fluorescent dye-conjugated second antibody and an Odyssey infrared imaging system (LI-COR Biosciences, Lincoln, NE) were used for the detection. The relative expression level was quantified using ImageQuant TL Image Analysis software (GE Healthcare).

Flutamide Hydrolase Activity. The flutamide hydrolase activity was determined as follows: a typical incubation mixture (final volume of 0.2 ml) contained 100 mM potassium phosphate buffer, pH 7.4, and various enzyme sources (human microsomal protein and COS7 cell homogenate expressing esterases, 0.4 mg/ml; human cytosolic protein, 1.0 mg/ml). In the preliminary study, we confirmed that the rate of formation of FLU-1 was linear with respect to the protein concentrations (<1.0 mg/ml human microsomal protein and COS7 cells homogenate expressing esterases and <1.5 mg/ml human cytosolic protein) and incubation time (<60 min). Flutamide was dissolved in dimethyl sulfoxide (DMSO), and the final concentration of DMSO in the incubation mixture was 1.0%. The reaction was initiated by the addition of 25 to 750 μM flutamide after 2-min preincubation at 37°C. After the 30-min incubation at 37°C, the reaction was terminated by the addition of 0.1 ml of ice-cold acetonitrile. After removal of the protein by centrifugation at 9500*g* for 5 min, a 60-μl portion of the supernatant was subjected to high-performance liquid chromatography (HPLC). The HPLC analysis was performed using an L-7100 pump (Hitachi, Tokyo, Japan), an L-7200 autosampler (Hitachi), an L-7405 UV detector (Hitachi), and a D-2500 Chromato-Integrator (Hitachi) equipped with a Mightysil RP-18 C18 GP column (5-μm particle size, 4.6 mm i.d.×150 mm; Kanto Chemical, Tokyo, Japan). The eluent was monitored at 376 nm with a noise-base clean Uni-3 (Union, Gunma, Japan), which can reduce the noise by integrating the output and increase the signal 3-fold by differentiating the output, and 5-fold by further amplification with an internal amplifier, resulting in a maximum 15-fold amplification of the signal. The mobile phase was 45% acetonitrile containing 25 mM ammonium acetate, pH 5.0. The flow rate was 1.0 ml/min. The column temperature was 35°C. The quantification of FLU-1 was performed by comparing the HPLC peak height with that of an authentic standard. Because FLU-1 contaminants exist in the commercially available flutamide to the extent of ~0.5%, the content of FLU-1 in the mixture incubated without the enzyme was subtracted from that with the enzyme to correct the activity. The activity in each concentration was determined as the mean value in triplicate. For kinetic analyses of flutamide hydrolase activity, the parameters were estimated from the fitted curves using a computer program (KaleidaGraph, Synergy Software, Reading, PA) designed for nonlinear regression analysis.

To clarify the involvement of various esterases, inhibition analysis of flutamide hydrolysis was performed by using representative esterase inhibitors. Organophosphates such as BNPP and DFP are known as general CES inhibitors (Heymann and Krisch, 1967; Yamaori et al., 2006). Eserine and NaF are cholinesterase inhibitors (Iwatsubo, 1965; Preuss and Svensson, 1996). EDTA is a paraoxonase inhibitor (Gonzalvo et al., 1997). PMSF is a serine hydrolase inhibitor (Johnson and Moore, 2000). Because heavy metals are frequently used for esterase inhibition studies, $AgNO_3$, $CdCl_2$, $CoCl_2$, and $CuCl_2$ were also used as inhibitors. Disulfiram was reported as a monoacylglycerol lipase inhibitor (Labar et al., 2007). The concentration of BNPP and DFP ranged from 0.001 to 1 mM, and that of the others was 0.1 and 1 mM. PMSF and disulfiram were dissolved in DMSO such that the final concentration of DMSO in the incubation mixture was 1.5%. Other inhibitors were dissolved in distilled water. The experimental procedure and condition were the same as above except that 500 μM flutamide was added. It was confirmed that 1.5% DMSO did not inhibit the flutamide hydrolase activity, and the control activity was determined in the presence of 1.5% DMSO.

***p*-Nitrophenyl Acetate Hydrolase Activity.** To confirm whether the recombinant AADAC, CES1, and CES2 are enzymatically active, the PNPA, a general esterase substrate, hydrolase activity was measured. The PNPA hydrolase activity was determined as follows: a typical incubation mixture was the same as above. PNPA was dissolved in DMSO, and the final concentration of DMSO in the incubation mixture was 1.0%. The reaction was initiated by the addition of 500 μM PNPA after 2-min preincubation at 37°C. After 5-min incubation at 37°C, the reaction was terminated by the addition of 0.1 ml of ice-cold methanol. The PNPA hydrolase activity was measured by the absorbance at 405 nm using Biotrak II plate reader (GE Healthcare). The quantification of *p*-nitrophenol, a metabolite of PNPA hydrolysis, was performed by comparing the absorbance with that of an authentic standard. Because *p*-nitrophenol contaminants exist in the commercially available PNPA to the extent of ~5%, the content of *p*-nitrophenol in the mixture incubated without the enzyme was subtracted from that with the enzyme to correct the activity.

Statistical Analysis. Comparison of two groups was made with unpaired, two-tailed Student's *t* test. Correlation analyses were performed by Spearman rank method. A value of $p < 0.05$ was considered statistically significant.

Results

PNPA and Flutamide Hydrolase Activities by Recombinant Human AADAC Wild-Type, AADAC Variant, CES1A1, CES1A2, and CES2. To compare the flutamide hydrolase activity between human AADAC, CES1A1, CES1A2, and CES2, they were transiently expressed in COS7 cells. The AADAC variant was also transiently expressed in COS7 cells. The protein expression levels were determined by immunoblot analysis (Fig. 1A). AADAC protein was specifically expressed in COS7 cells transfected with the expression plasmids of AADAC wild-type and variant. CES1A and CES2 proteins were specifically expressed in COS7 cells transfected with the expression plasmids of CES1A1 or CES1A2, and CES2, respectively. To confirm that these enzymes were enzymatically active, PNPA hydrolase activity was measured at a concentration of 500 μM PNPA (Fig. 1B). The recombinant CES2A1 showed the highest PNPA hydrolase activity (621 ± 61 nmol/min/mg protein), and the recombinant AADAC wild-type, variant, CES1A1, and CES1A2 showed similar activities (243 ± 11, 247 ± 24, 293 ± 19, and 245 ± 18 nmol/min/mg protein, respectively). The flutamide hydrolase activities were determined at a concentration of 500 μM flutamide (Fig. 1C). Among them, the AADAC wild-type and variant showed flutamide hydrolase activity (0.28 ± 0.03 and 0.30 ± 0.01 nmol/min/mg protein, respectively). In contrast, CES1A1, CES1A2, and CES2 showed almost no activity (0.003 ± 0.003, 0.008 ± 0.008, and 0.012 ± 0.007 nmol/min/mg protein, respectively), similar to mock COS7 cells (0.012 ± 0.007 nmol/min/mg protein). These results suggested that AADAC, but not the CES enzymes, contributed to the flutamide hydrolysis.

Kinetic Analyses of Flutamide Hydrolase Activity by HLM, HLC, and Recombinant Human AADAC. It was previously suggested that AADAC is localized to the endoplasmic reticulum lumen (Frick et al., 2004). Therefore, it is assumed that flutamide can be hydrolyzed in HLM rather than in HLC. In this study, the flutamide hydrolase activity in HLM and HLC was measured (Fig. 2A). The maximum concentration was 750 μM because of the limited solubility of flutamide in the incubation mixture. For HLM, the K_m and V_{max} values were 794 ± 83 μM and 1.1 ± 0.0 nmol/min/mg protein, respectively, resulting in an intrinsic clearance of 1.4 ± 0.1 μl/min/mg protein. For HLC, because the flutamide hydrolase activity ranging from 25 to 750 μM was linear, the K_m and V_{max} values could not be calculated by the Michaelis-Menten equation. The K_m value of the flutamide hydrolase activity by HLC appeared to be substantially higher than that by HLM. These results suggested that the contribution to flutamide hydrolysis by HLM was much higher than that by HLC. In addition, kinetic analyses of the flutamide hydrolase activity by the recombinant AADAC wild-type and variant were also performed (Fig. 2B). The K_m and V_{max} values of the AADAC wild-type were 778 ± 122 μM and 0.6 ± 0.1 nmol/min/mg

DMD DRUG METABOLISM AND DISPOSITION aspet

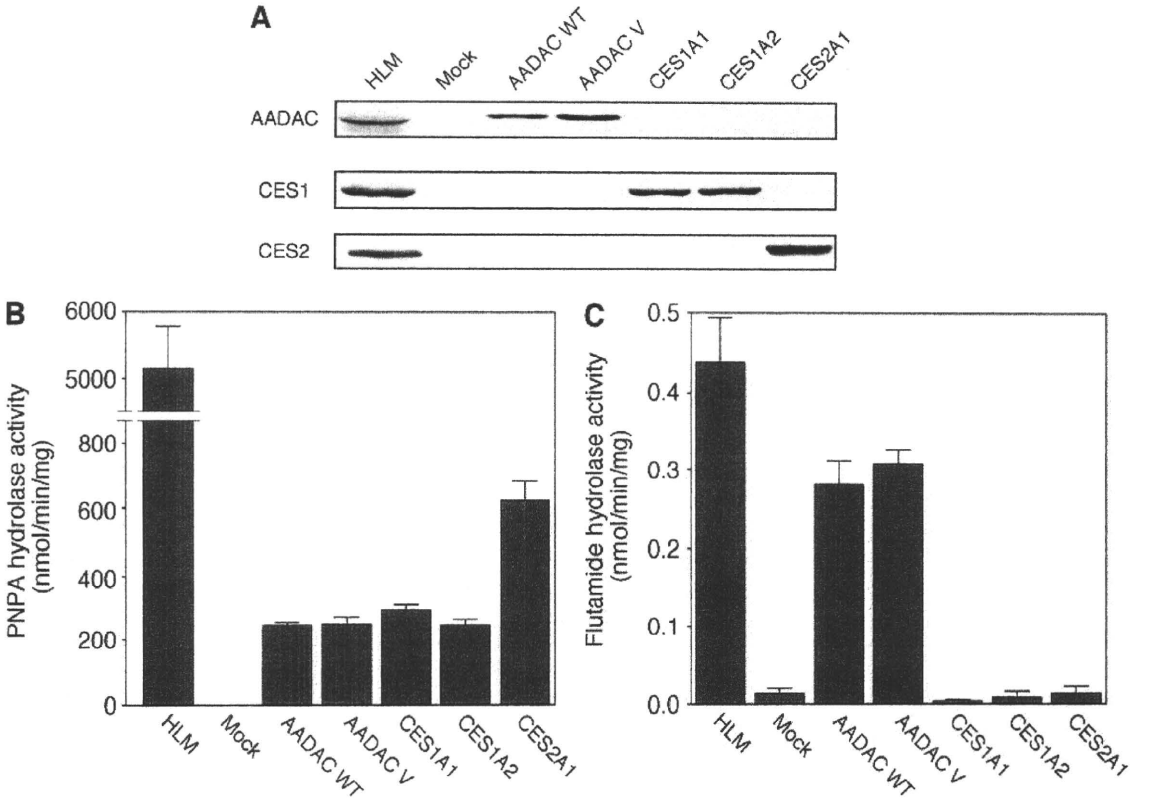

FIG. 1. A, immunoblot analysis of recombinant human AADAC, CES1, and CES2 expressed in COS7 cells. Total cell homogenates from COS7 cells (30 μg) were separated by electrophoresis using 10% SDS-polyacrylamide gel. PNPA hydrolase activities (B) and flutamide hydrolase activities (C) by recombinant AADAC, CES1, and CES2. The homogenates of COS7 cells expressing these enzymes were incubated with 100 μM PNPA or 500 μM flutamide. Each column represents the mean ± S.D. of triplicate determinations. WT, wild type; V, variant.

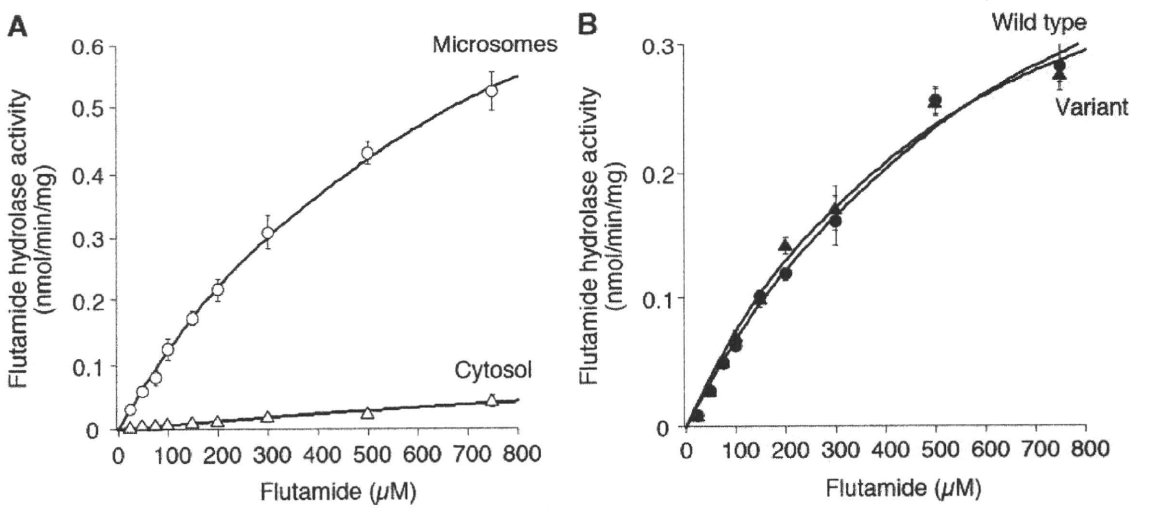

FIG. 2. Kinetic analyses of flutamide hydrolase activities in HLM and HLC (A) and by the recombinant AADAC wild-type and variant (B). The kinetic parameters were estimated from the fitted curve using the computer program KaleidaGraph designed for nonlinear regression analysis. Each data point represents the mean ± S.D. of triplicate determination.

protein, respectively, resulting in an intrinsic clearance of 0.8 ± 0.0 μl/min/mg protein. The K_m and V_{max} values of the AADAC variant were 591 ± 75 μM and 0.5 ± 0.0 nmol/min/mg protein, respectively, resulting in an intrinsic clearance of 0.9 ± 0.1 μl/min/mg protein. Thus, the AADAC variant did not alter the flutamide hydrolase activity. In addition, the K_m values of HLM and AADAC wild-type were not significantly different. These results suggested that AADAC was involved in flutamide hydrolysis in human liver.

Effects of Chemical Inhibitors on Flutamide Hydrolase Activity in HLM and Recombinant AADAC. To prove that AADAC is a principal enzyme for flutamide hydrolysis in human liver, the effects of inhibitors on the flutamide hydrolase activities by HLM and the

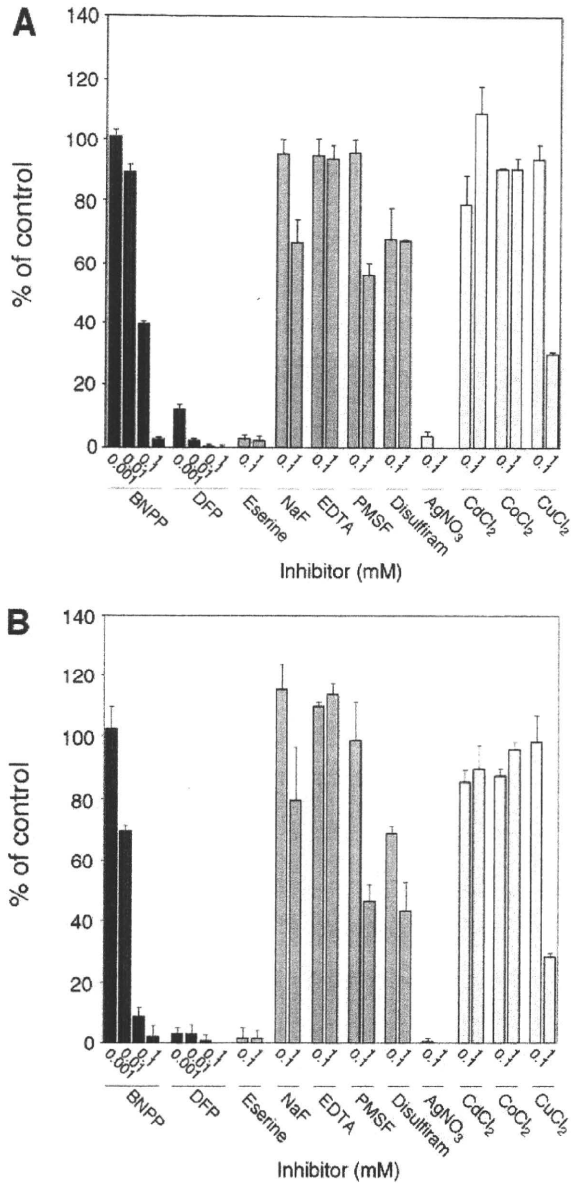

FIG. 3. Effects of chemical inhibitors on flutamide hydrolase activity. Flutamide hydrolase activities in HLM (A) and the recombinant AADAC (B) wild-type were determined at a substrate concentration of 500 μM. The control activity values were 0.438 (A) and 0.283 (B) nmol/min/mg protein, respectively. Each column represents the mean ± S.D. of triplicate determinations.

recombinant AADAC were analyzed. In this study, representative inhibitors of various esterases were used to clarify the involvement of various esterases and examine the inhibitory characteristics of AADAC. The flutamide hydrolase activity by HLM was inhibited in a BNPP concentration-dependent manner and was potently inhibited by 0.01 to 1 mM DFP, 0.1 to 1 mM eserine, and $AgNO_3$ (Fig. 3A). In addition, the flutamide hydrolase activity by HLM was moderately inhibited by 1 mM NaF, PMSF, disulfiram, and $CuCl_2$. However, no inhibition occurred by EDTA, $CaCl_2$, and $CoCl_2$. A similar inhibition pattern was obtained by the recombinant AADAC wild-type (Fig. 3B) and variant (data not shown). These results imply that AADAC is a major esterase responsible for the flutamide hydrolysis in human liver.

Expression of AADAC mRNA in Human Normal Tissues. The expression level of AADAC mRNA in human tissues was determined by

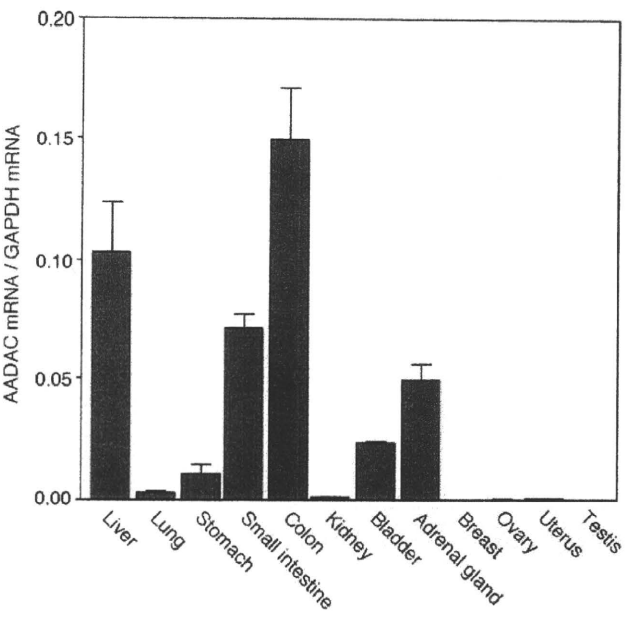

FIG. 4. Expression levels of AADAC mRNA in various human normal tissues. Relative copy numbers of AADAC to GAPDH in human tissues were determined by real-time RT-PCR analysis. Each column represents the mean ± S.D. of triplicate determinations.

real-time RT-PCR analysis (Fig. 4). The expression level of AADAC mRNA was normalized with GAPDH mRNA level. AADAC mRNA is highly expressed in colon, liver, and small intestine and moderately expressed in adrenal gland, bladder, and stomach. Other tissues investigated in this study showed low expression levels. We previously examined the expressions of CES1A1, CES1A2, and CES2 mRNA in human normal tissues (T. Maruichi, M. Katoh, S. Takahashi, M. Nakajima, and T. Yokoi, unpublished data). The expression levels of AADAC mRNA in all the tissues except colon and adrenal gland were lower than those of these CES mRNA. The expression level of AADAC in human liver was 116-, 23-, and 8-fold lower than those of CES1A1, CES1A2, and CES2, respectively.

Expression of AADAC Protein and Flutamide Hydrolase Activities in Human Tissues. To further analyze whether AADAC is responsible for the flutamide hydrolysis in humans, the expression of AADAC and the flutamide hydrolase activity in various human tissues were measured. The expression levels of AADAC, CES1A, and CES2 proteins in HLM, HJM, HPM, and HRM were determined by immunoblot analysis (Fig. 5A). AADAC protein was expressed in HLM and HJM but not in HPM and HRM. This result corresponded with the expression of AADAC mRNA (Fig. 4). CES1A protein was expressed in HLM and HPM, whereas CES2 protein was expressed in HLM, HJM, and HRM. High flutamide hydrolase activity at a concentration of 500 μM flutamide was detected in HJM (0.72 ± 0.02 nmol/min/mg protein) and HLM (0.43 ± 0.03 nmol/min/mg protein). The fact that the hydrolase activity in HJM was higher than that in HLM was supported by the results of the immunoblot analysis. On the other hand, HPM, in which CES1A is expressed, and HRM, in which CES2 is expressed, showed slight hydrolase activity (0.02 ± 0.00 and 0.01 ± 0.01 nmol/min/mg protein, respectively). These results suggested that AADAC is responsible for the flutamide hydrolysis in humans.

Correlation Analysis between Flutamide Hydrolase Activity and AADAC Protein Expression Level. The flutamide hydrolase activities in microsomes from 50 human livers were determined at a concentration of 500 μM. The flutamide hydrolase activities ranged

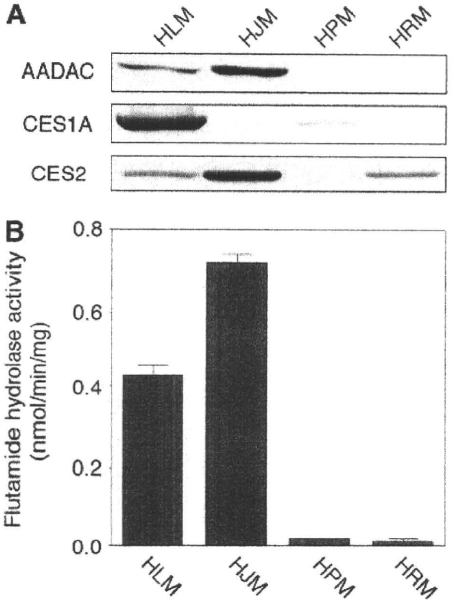

FIG. 5. A, immunoblot analysis of AADAC, CES1A, and CES2 in HLM, HJM, HPM, and HRM. Total cell homogenates from COS7 cells (30 μg) were separated by electrophoresis using 10% SDS-polyacrylamide gel. B, flutamide hydrolase activities in microsomes. The microsomes were incubated with 500 μM flutamide. Each column represents the mean ± S.D. of triplicate determinations.

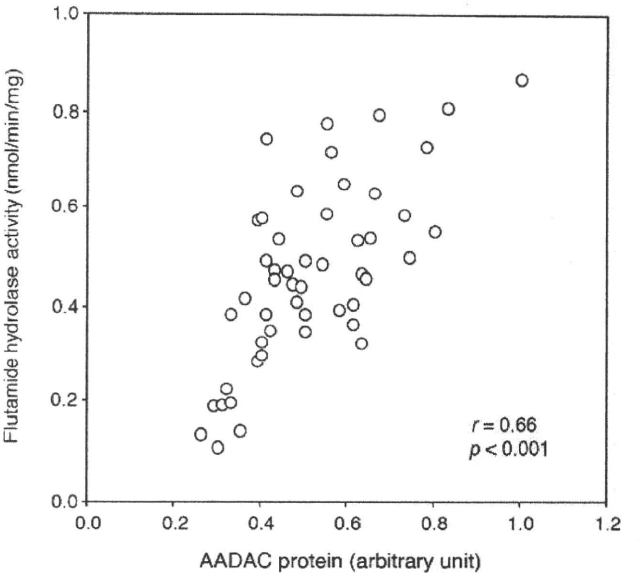

FIG. 6. Correlation between the expression levels of AADAC protein and flutamide hydrolase activities in 50 HLM. The expression level of AADAC protein was determined by immunoblot analysis. The flutamide hydrolase activity was determined by HPLC.

from 0.11 to 0.87 nmol/min/mg protein (mean ± S.D., 0.47 ± 0.19 nmol/min/mg protein), resulting in 7.9-fold interindividual variability. In addition, the expression levels of AADAC protein in microsomes from 50 human livers were determined by immunoblot analysis. The AADAC protein expression levels are represented as relative levels to the sample, which is the highest expression level. The relative expression levels of AADAC protein in HLM ranged from 0.26 to 1.00, resulting in 3.8-fold interindividual variability. As shown in Fig. 6, the expression level of AADAC protein and the flutamide hydrolase activity were significantly correlated ($r = 0.66$, $p < 0.001$). These results also supported that AADAC is a principal enzyme for the flutamide hydrolysis.

Discussion

Human AADAC was first identified as an enzyme that catalyzes the deacetylation of 2-acetylaminofluorene (Probst et al., 1991). It has been believed that AADAC might function as a lipase because of the high homology of the active site of AADAC with that of hormone-sensitive lipase (Probst et al., 1994). On the other hand, human CES enzymes are major serine esterases involved in the hydrolysis of various drugs and xenobiotics. AADAC is one of the major serine esterases expressed in HLM and CES enzymes (Ross and Crow, 2007), but it was unknown whether AADAC is involved in the hydrolysis of therapeutic drugs.

An antiandrogen drug, flutamide, has been widely used for prostate cancer, but severe hepatotoxicity sometimes occurred. Several studies suggested that the flutamide-induced hepatotoxicity was caused by FLU-1, a metabolite of hydrolyzed flutamide, or *N*-hydroxyl FLU-1, a metabolite of FLU-1 by CYP3A or CYP1A (Aizawa et al., 2003; Matsuzaki et al., 2006; Ohbuchi et al., 2009). Therefore, it was considered that flutamide hydrolysis was important in the occurrence of hepatotoxicity, but the flutamide hydrolase enzyme had never been identified. It was conceivable that human CES enzymes CES1A and CES2 are responsible for the hydrolysis of flutamide because they contribute largely to the hydrolysis of various drugs and xenobiotics. However, it was reported that the flutamide hydrolase activity was not detected by using purified CES1A and CES2 (Takai et al., 1997), which is consistent with our finding that the recombinant CES1A1, CES1A2, and CES2A1 did not show the flutamide hydrolase activity (Fig. 1C). Moreover, the activity was scarcely detected in HPM and HRM, in which CES1A and CES2 enzymes were expressed, respectively. On the other hand, the recombinant AADAC showed the flutamide hydrolase activity, and the activity was highly detected in HLM and HJM, in which AADAC is expressed. Furthermore, the similar activities of flutamide hydrolysis in HLM and the recombinant AADAC were consistent with the similar blot densities of AADAC (Fig. 1, A and C). Thus, we found that human AADAC is a major contributor to the flutamide hydrolysis. PNPA hydrolase activity, a general esterase activity, was detected in recombinant AADAC and CES1A1, CES1A2, and CES2A1 (Fig. 1B). However, the activity in HLM was substantially higher than the sum of those by recombinant AADAC and CES enzymes (Fig. 1B). Other esterases such as paraoxonase and butyrylcholinesterase may participate in the PNPA hydrolysis in HLM.

It has been reported that AADAC is located on the lumen side of endoplasmic reticulum (Frick et al., 2004). This corresponded to the present result that the flutamide hydrolase activity in HLM was substantially higher than in HLC (Fig. 2A). In addition, there was no significant difference between the K_m values of HLM (794 ± 83 μM) and recombinant AADAC wild-type (778 ± 122 μM) (Fig. 2, A and B). This finding also supported the involvement of AADAC in flutamide hydrolysis in human liver. However, the activity was also detected in HLC. It was already known that CES1A and CES2 enzymes are present in HLC (Xu et al., 2002; Tabata et al., 2004), but recombinant CES1A1, CES1A2, and CES2 could not hydrolyze flutamide (Fig. 1C). In addition, it was shown that sialic acid 9-*O*-acetylesterase, an alacepril hydrolase enzyme, purified from rat liver cytosol also could not hydrolyze flutamide (Usui et al., 2003). Therefore, other enzymes that can hydrolyze flutamide may be present in HLC, but the contribution to flutamide hydrolysis would be limited.

To confirm that flutamide hydrolysis in HLM is specifically cata-

lyzed by AADAC, we performed inhibition analyses by using various chemical inhibitors and heavy metals (Fig. 3). The flutamide hydrolase activity in HLM was inhibited in a BNPP concentration-dependent manner but was not completely inhibited by 1 mM PMSF (residual activity, 56% of control). It is known that the CES1A and CES2 enzyme activities are inhibited in a BNPP concentration-dependent manner and were substantially inhibited by 0.1 mM PMSF (Xie et al., 2002). Therefore, these enzymes would not contribute to the flutamide hydrolysis in HLM. Moreover, the activity was potently inhibited by DFP, eserine, and silver nitrate and moderately inhibited by NaF, disulfiram, and $CuCl_2$. Other inhibitors used in the present study did not cause inhibition. Because DFP and BNPP are organophosphates, general CES inhibitors, it is plausible that DFP also inhibits AADAC. Eserine and NaF are cholinesterase inhibitors (Iwatsubo, 1965; Ciliv and Ozand, 1972; Preuss and Svensson, 1996). It is of interest that flutamide hydrolysis was effectively inhibited by eserine but not by NaF. EDTA and disulfiram are known to be inhibitors of paraoxonase and monoacylglycerol lipase, respectively (Gonzalvo et al., 1997; Labar et al., 2007). Therefore, it was conceivable that these enzymes did not contribute to the flutamide hydrolysis in HLM. The inhibitory specificity of esterases by heavy metals has not been obvious, but in this study we found that AADAC was potently inhibited by $AgNO_3$ and moderately inhibited by $CuCl_2$. Probst et al. (1994) previously reported that the 2-acetylaminofluorene deacetylation catalyzed by AADAC in HLM was inhibited in a BNPP concentration-dependent manner but was not inhibited by increasing the concentrations of PMSF. The inhibition pattern of flutamide hydrolysis by BNPP and PMSF was similar to that of 2-acetylaminofluorene deacetylation.

To investigate the tissue distribution of AADAC mRNA in human normal tissues, real-time RT-PCR was performed (Fig. 4). AADAC mRNA was mainly expressed in human normal liver, small intestine, and colon. In addition, we confirmed that AADAC protein was expressed in human liver and jejunum microsomes but not in human pulmonary and renal microsomes (Fig. 5A). The tissue distribution of AADAC protein corresponded to that of AADAC mRNA. It is of interest that the expression of AADAC protein in jejunum was higher than in liver, although the mRNA expression was opposite. As shown in Fig. 6, there was interindividual variability in AADAC protein level and flutamide hydrolase activity in human liver. The discrepancy may be because of use of liver RNA derived from single donor. In general, the small intestine plays an important role in the first-pass metabolism of therapeutic drugs given orally (Lin et al., 1999). AADAC would play a certain role in the first-pass metabolism of flutamide in small intestine and in liver.

Correlation analysis was performed between the expression level of AADAC protein and the flutamide hydrolase activity using individual HLM samples (Fig. 6). The correlation between the expression level of AADAC and the flutamide hydrolase activity was strongly significant. Although the point appears to show an *x*-axis intercept greater than 0, several individual HLM samples may partially include inactive AADAC protein. The expression level of AADAC protein and the flutamide hydrolase activity were moderately variable. It is feasible that the induction by xenobiotics from the environment or diet and endobiotics, and genetic polymorphism of the *AADAC* gene affect the interindividual variability of the flutamide hydrolase activity and AADAC expression level. However, the regulation mechanisms of human AADAC expression are not fully understood. Saito et al. (2003) previously found 23 SNPs in the *AADAC* gene using DNA samples of 48 Japanese. Among them, only an SNP that was also found in this study (g.13651G > A, c.931G > A) leads to an amino acid change (V281I). However, AADAC variant (V281I) appeared not to alter the enzyme activity (Fig. 3B). It is considered that flutamide hydrolysis is important in the occurrence of hepatotoxicity (Aizawa et al., 2003; Matsuzaki et al., 2006; Ohbuchi et al., 2009). Therefore, the interindividual variability of AADAC might affect the incidence of flutamide-induced hepatotoxicity. Further study on the regulation mechanisms and genetic polymorphisms of human AADAC will be necessary.

In conclusion, we found that human AADAC is a principal enzyme in the flutamide hydrolysis. The present study is the first report of the contribution of human AADAC to the metabolism of a therapeutic drug.

Acknowledgments. We thank Brent Bell for review of the manuscript.

References

Aizawa Y, Ikemoto I, Kishimoto K, Wada T, Yamazaki H, Ohishi Y, Kiyota H, Furuta N, Suzuki H, and Ueda M (2003) Flutamide-induced hepatic dysfunction in relation to steady-state plasma concentrations of flutamide and its metabolites. *Mol Cell Biochem* **252:**149–156.

Block W and Arndt R (1978) Chromatographic study on the specificity of bis-*p*-nitrophenylphosphate in vivo. Identification of labelled proteins of rat liver after intravenous injection of bis-*p*-nitro[14C]phenylphosphate as carboxylesterases and amidases. *Biochim Biophys Acta* **524:**85–93.

Ciliv G and Ozand PT (1972) Human erythrocyte acetylcholinesterase purification, properties and kinetic behavior. *Biochim Biophys Acta* **284:**136–156.

Crawford ED, Eisenberger MA, McLeod DG, Spaulding JT, Benson R, Dorr FA, Blumenstein BA, Davis MA, and Goodman PJ (1989) A controlled trial of leuprolide with and without flutamide in prostatic carcinoma. *N Engl J Med* **321:**419–424.

Fau D, Eugene D, Berson A, Letteron P, Fromenty B, Fisch C, and Pessayre D (1994) Toxicity of the antiandrogen flutamide I isolated rat hepatocytes. *J Pharmacol Exp Ther* **269:**954–962.

Frick C, Atanasov AG, Arnold P, Ozols J, and Odermatt A (2004) Appropriate function of 11β-hydroxysteroid dehydrogenase type 1 in the endoplasmic reticulum lumen is dependent on its N-terminal region sharing similar topological determinants with 50-kDa esterase. *J Biol Chem* **279:**31131–31138.

Goda R, Nagai D, Akiyama Y, Nishikawa K, Ikemoto I, Aizawa Y, Nagata K, and Yamazoe Y (2006) Detection of new *N*-oxidized metabolite of flutamide, *N*-[4-nitro-3-(trifluoromethyl) phenyl]hydroxylamide, in human liver microsomes and urine of prostate cancer patients. *Drug Metab Dispos* **34:**828–835.

Gonzalvo MC, Gil F, Hernández AF, Villanueva E, and Pla A (1997) Inhibition of paraoxonase activity in human liver microsomes by exposure to EDTA, metals and merculials. *Chem Biol Interact* **105:**169–179.

Heymann E and Krisch K (1967) Phospholic acid-bis-(*p*-nitro-phenylester), a new inhibitor of microsomal carboxylesterases. *Hoppe Seylers Z Physiol Chem* **348:**609–619.

Imai T, Taketani M, Shii M, Hosokawa M, and Chiba K (2006) Substrate specificity of carboxylesterase isozymes and their contribution to hydrolase activity in human liver and small intestine. *Drug Metab Dispos* **34:**1734–1741.

Iwatsubo K (1965) Studies on the classification of the enzymes hydrolysing ester-form drugs in liver microsomes. *Jpn J Pharmacol* **15:**244–265.

Johnson G and Moore SW (2000) Cholinesterase-like catalytic antibodies: reaction with substrates and inhibitors. *Mol Immunol* **37:**707–719.

Katchen B and Buxbaum S (1975) Disposition of a new, nonsteroid, antiandrogen, alpha,alpha,alpha-trifluoro-2-methyl-4′-nitro-m-propionotoluidine (Flutamide), in men following a single oral 200 mg dose. *J Clin Endocrinol Metab* **41:**373–379.

Labar G, Bauvois C, Muccioli GG, Wouters J, and Lambert DM (2007) Disulfiram is an inhibitor of human purified monoacylglycerol lipase, the enzyme regulating 2-arachidonoylglycerol signaling. *Chembiochem* **8:**1293–1297.

Laemmli UK (1970) Cleavage of structural proteins during the assembly of the head of bacteriophage T4. *Nature* **227:**680–685.

Lin JH, Chiba M, and Baillie TA (1999) Is the role of the small intestine in first-pass metabolism overemphasized? *Pharmacol Rev* **51:**135–158.

Matsuzaki Y, Nagai D, Ichimura E, Goda R, Tomura A, Doi M, and Nishikawa K (2006) Metabolism and hepatic toxicity of flutamide in cytochrome P450 1A2 knockout SV129 mice. *J Gastroenterol* **41:**231–239.

Mentlein R, Rix-Matzen H, and Heymann E (1988) Subcellular localization of non-specific carboxylesterases, acylcarnitine hydrolase, monoacylglycerol lipase and palmitoyl-CoA hydrolase in rat liver. *Biochim Biophys Acta* **964:**319–328.

Nakajima M, Itoh M, Sakai H, Fukami T, Katoh M, Yamazaki H, Kadlubar FF, Imaoka S, Funae Y, and Yokoi T (2006) CYP2A13 expressed in human bladder metabolically activates 4-aminobiphenyl. *Int J Cancer* **119:**2520–2526.

Ohbuchi M, Miyata M, Nagai D, Shimada M, Yoshinari K, and Yamazoe Y (2009) Role of enzymatic *N*-hydroxylation and reduction in flutamide metabolite-induced liver toxicity. *Drug Metab Dispos* **37:**97–105.

Ozono S, Yamaguchi A, Mochizuki H, Kawakami T, Fujimoto K, Otani T, Yoshida K, Ichinei M, Yamashita T, and Hirao Y (2002) Caffeine test in predicting flutamide-induced hepatic injury in patients with prostate cancer. *Prostate Cancer Prostatic Dis* **5:**128–131.

Preuss CV and Svensson CK (1996) Arylacetamide deacetylase activity towards monoacetyldapsone. *Biochem Pharmacol* **51:**1661–1668.

Probst MR, Beer M, Beer D, Jenö P, Meyer UA, and Gasser R (1994) Human liver arylacetamide deacetylase. Molecular cloning of a novel esterase involved in the metabolic activation of arylamine carcinogens with high sequence similarity to hormone-sensitive lipase. *J Biol Chem* **269:**21650–21656.

Probst MR, Jenö P, and Meyer UA (1991) Purification and characterization of a human liver arylacetamide deacetylase. *Biochem Biophys Res Commun* **177:**453–459.

Ross MK and Crow JA (2007) Human carboxylesterases and their role in xenobiotic and endobiotic metabolism. *J Biochem Mol Toxicol* **21:**187–196.

Saito S, Iida A, Sekine A, Kawauchi S, Higuchi S, Ogawa C, and Nakamura Y (2003) Catalog of 680 variations among eight cytochrome P450 (CYP) genes, nine esterase genes, and two other genes in the Japanese population. *J Hum Genet* **48:**249–270.

Sanghani SP, Quinney SK, Fredenburg TB, Davis WI, Murry DJ, and Bosron WF (2004) Hydrolysis of irinotecan and its oxidative metabolites, 7-ethyl-10-[4-N-(5-aminopentanoic acid)-1-piperidino] carbonyloxycamptothecin and 7-ethyl-10-[4-(1-piperidino)-1-amino]-carbonyloxycamptothecin, by human carboxylesterases CES1A1, CES2, and a newly expressed carboxylesterase isoenzyme, CES3. *Drug Metab Dispos* **32:**505–511.

Schulz M, Schmoldt A, Donn F, and Becker H (1988) The pharmacokinetics of flutamide and its metabolites after a single oral dose and during chronic treatment. *Eur J Clin Pharmacol* **34:**633–636.

Tabata T, Katoh M, Tokudome S, Hosakawa M, Chiba K, Nakajima M, and Yokoi T (2004) Bioactivation of capecitabine in human liver: involvement of the cytosolic enzyme on 5′-deoxy-5-fluorocytidine formation. *Drug Metab Dispos* **32:**762–767.

Takai S, Matsuda A, Usami Y, Adachi T, Sugiyama T, Katagiri Y, Tatematsu M, and Hirano K (1997) Hydrolytic profile for ester- or amide-linkage by carboxylesterases pI 5.3 and 4.5 from human liver. *Biol Pharm Bull* **20:**869–873.

Thole Z, Manso G, Salgueiro E, Revuelta P, and Hidalgo A (2004) Hepatotoxicity induced by antiandrogens: a review of the literature. *Urol Int* **73:**289–295.

Tiwari R, Köffel R, and Schneiter R (2007) An acetylation/deacetylation cycle controls the export of sterols and steroids from. *S. cerevisiae. EMBO J* **26:**5109–5119.

Tsuchiya Y, Nakajima M, Kyo S, Kanaya T, Inoue M, and Yokoi T (2004) Human CYP1B1 is regulated by estradiol via estrogen receptor. *Cancer Res* **64:**3119–3125.

Usui S, Kubota M, Iguchi K, Kiho T, Sugiyama T, Katagiri Y, and Hirano K (2003) Sialic acid 9-*O*-acetylesterase catalyzes the hydrolyzing reaction from alacepril to deacetylalacepril. *Pharm Res* **20:**1309–1316.

Xie M, Yang D, Liu L, Xue B, and Yan B (2002) Human and rodent carboxylesterase: immunorelatedness, overlapping substrate specificity, differential sensitivity to serine enzyme inhibitors, and tumor-related expression. *Drug Metab Dispos* **30:**541–547.

Xu G, Zhang W, Ma MK, and McLeod HL (2002) Human carboxylesterase 2 is commonly expressed in tumor tissue and is correlated with activation of irionotecan. *Clin Cancer Res* **8:**2605–2611.

Yamaori S, Fujiyama N, Kushihara M, Funahashi T, Kimura T, Yamamoto I, Sone T, Isobe M, Ohshima T, Matsumura K, et al. (2006) Involvement of human blood arylesterases and liver microsomal carboxylesterases in nafamostat hydrolysis. *Drug Metab Pharmacokinet* **21:**147–155.

Address correspondence to: Tsuyoshi Yokoi, Drug Metabolism and Toxicology, Faculty of Pharmaceutical Sciences, Kanazawa University, Kakuma-machi, Kanazawa 920-1192, Japan. E-mail: tyokoi@kenroku.kanazawa-u.ac.jp

Doi: 10.1111/j.1742-7843.2009.00410.x
Journal compilation © 2009 Nordic Pharmacological Society. *Basic & Clinical Pharmacology & Toxicology*, **105**, 156–166

Identification of Urinary Biomarkers Useful for Distinguishing a Difference in Mechanism of Toxicity in Rat Model of Cholestasis

Kenji Ishihara[1], Naruo Katsutani[2], Naoki Asai[3], Akira Inomata[1], Yuji Uemura[1], Akiyoshi Suganuma[1], Kohei Sawada[1], Tsuyoshi Yokoi[4] and Toyohiko Aoki[2]

[1]Tsukuba Research, Drug Safety Research Laboratories, Eisai Co., Ltd., Tsukuba, Japan, [2]Kawashima Research, Drug Safety Research Laboratories, Eisai Co., Ltd., Kakamigahara, Japan, [3]Tsukuba Research, Analytical Research Laboratories, Eisai Co., Ltd., Tsukuba, Japan, and [4]Drug Metabolism and Toxicology, Division of Pharmaceutical Sciences, Graduate School of Medical Science, Kanazawa University, Kanazawa, Japan

(Received 19 November 2008; Accepted 14 January 2009)

Abstract: This ^{1}H nuclear magnetic resonance metabonomics study was aimed to determine urinary biomarkers of cholestasis resulting from inhibition of biliary secretion of bile or obstruction of bile flow. To inhibit biliary secretion of bile, cyclosporine A was administered to male Sprague–Dawley rats. Obstruction of bile flow was induced by administration of 4,4′-methylene dianiline, α-naphthylisothiocyanate or bile duct ligation. Clinical pathological and histopathological examinations were performed to confirm cholestatic injury and ^{1}H nuclear magnetic resonance spectral data for urine samples were analysed to determine similarities and differences in profiles of metabolites using the Spotfire®. In cyclosporine A-treated groups, serum total bilirubin and bile acid were significantly increased but no remarkable hepatic histopathological-changes were observed. In 4,4′-methylene dianiline-, α-naphthylisothiocyanate- and bile duct ligation-treated groups, serum alkaline phosphatase, γ-glutamyltranspeptidase and total bilirubin levels increased significantly, and hepatic histopathological-changes were observed. On urinary ^{1}H nuclear magnetic resonance spectral analysis, area intensities derived from 0.66 to 1.90 ppm were decreased by cyclosporine A, whereas they were increased by other treatments. These metabolites were identified using the NMR suite® as bile acids, branched-chain amino acids, n-butyrate, propionate, methyl malonate and valerate. These metabolites were further investigated by K-means clustering analysis. The cluster of these metabolites is considered to be altered by cholestasis. We conclude that bile acids, valine and methyl malonate have a possibility to be urinary cholestatic biomarkers, which distinguish a difference in mechanism of toxicity. ^{1}H nuclear magnetic resonance metabonomics thus appears to be useful for determining the mechanisms of toxicity and can be front-loaded in drug safety evaluation and biomarker discovery.

Hepatotoxicity has been a major reason for failure in drug development, particularly for new drug candidates in the preclinical stage [1,2]. Hepatotoxicity characterized mainly by arrest of bile flow is termed cholestatic injury or intrahepatic cholestasis. A variety of chemical agents can cause cholestatic injury as an idiosyncratic reaction, either immunologically or metabolically. Some are intrinsic hepatotoxins, either synthetic or natural, that lead to impairment of bile flow as a dose-dependent toxic effect. Toxic or idiosyncratic injury can interfere with bile flow by selective injury or blockade of hepatic uptake, processing or excretion of the components of bile [3].

The causes of cholestasis are classified mainly into two types, based on whether the primary injury occurs intra-hepatically (in the biliary canaliculus) or extra-hepatically (in the bile ducts). Cholestasis occurring intra-hepatically is due to interaction of chemical agents or their metabolites with transporters for excretion of the bile [4,5], while cholestasis occurring extra-hepatically is due to impairment in bile flow at the bile duct level [6,7]. Clinically, the differential diagnosis of cholestasis requires ultrasonography in addition to blood chemistry analysis and urinalysis.

One of the advantages of ^{1}H nuclear magnetic resonance-based metabonomics is its ability to quickly and stably detect a wide range of metabolites with various physicochemical properties in biofluids [8,9]. It can thus provide information on changes in biological substances associated with cholestasis by a single measurement with clustering and pattern detection analysis [10]. ^{1}H nuclear magnetic resonance-based metabonomics can be used for a wide range of problems, including disease diagnosis, preclinical evaluation of candidate drugs in safety studies, assessment of safety in humans in clinical trials, and nutritional studies [11]. However, ^{1}H nuclear magnetic resonance-based metabonomics has not been successfully applied to early diagnosis of cholestasis, because the validity of biomarkers in urine has not been well-established.

In a previous ^{1}H nuclear magnetic resonance metabonomics study, we investigated and compared the biochemical profiles of metabolites in urine from rats treated with hepatotoxicants with different mechanisms of effect [12]. We used 4,4′-methylene dianiline as a model compound inducing bile duct injury, and clofibrate and galactosamine to produce models of

Author for correspondence: Kenji Ishihara, Tsukuba Research, Drug Safety Research Laboratories, Eisai Co., Ltd., 5-1-3 Tokodai, Tsukuba 300-2635, Japan (fax + 81 29 847 6931, e-mail k3-ishihara@hhc.eisai.co.jp).

peroxisome proliferation in the liver and hepatocyte death, respectively [12]. The most significant differences between the 4,4′-methylene dianiline-treated groups (250 mg/kg oral administration) and groups treated with other agents (clofibrate 500 mg/kg oral administration, galactosamine 500 mg/kg intraperitoneal administration) were observed in chemical shifts of peaks mainly between 0.66 and 1.90 ppm. These findings suggested that ^{1}H nuclear magnetic resonance analysis of these urinary metabolites may provide a powerful means of determination of the pathophysiological status of cholestasis induced by hepatotoxicants such as cyclosporine A, 4,4′-methylene dianiline and α-naphthylisothiocyanate.

The purpose of the present study was to determine whether ^{1}H nuclear magnetic resonance-based metabonomics using urine samples can discriminate differences in mechanism of toxicity after administration of chemical agents or treatment causing cholestatic injury. To inhibit biliary secretion of bile acid, cyclosporine A was administered to male Sprague–Dawley (Crl : CD(SD)) rats. Obstruction of bile flow was induced by administration of 4,4′-methylene dianiline or α-naphthylisothiocyanate. In addition, artificial cholestasis to obstruct bile flow was induced by bile duct ligation in rats. To identify putative metabolites associated with cholestasis, urine samples obtained were subjected to ^{1}H nuclear magnetic resonance analysis along with clinical pathological and histopathological examinations to confirm cholestatic injury.

Materials and Methods

Test materials and animal treatment. Cyclosporine A (Sandimmun®) as a solution (50 mg/ml) for intravenous administration was obtained from Novartis pharma (East Hanover, NJ, USA). For intraperitoneal administration, cyclosporine A was diluted with saline solution. 4,4′-methylene dianiline and α-naphthylisothiocyanate were obtained from Sigma-Aldrich (St Louis, MO, USA). They were suspended in 0.5% methylcellulose solution. All other reagents and chemicals for the nuclear magnetic resonance experiments and biochemical analyses were of the highest commercially available quality.

Fifty-six male Crl : CD(SD) rats (Charles River Japan, Shiga, Japan) were divided into a total of 12 groups, including 10 groups (n = 5) for cyclosporine A, 4,4′-methylene dianiline, α-naphthylisothiocyanate treatment and two groups (n = 3) for bile duct ligation. The animals were kept individually in metabolic cages at a temperature of 23 ± 3° with 55 ± 20% relative humidity and a 12 hr light/12 hr dark cycle with at least 10 air changes per hour. They were allowed to access solid CDF-1 rodent chow (Oriental Yeast, Tokyo, Japan) and water *ad libitum*.

At 8 weeks of age, four groups of rats of the same age received a single oral administration of 4,4′-methylene dianiline (50: minimum toxic dose [13], 100 or 250 mg/kg, n = 5) or vehicle (0.5% methylcellulose solution, n = 5) as control-1. Three groups of animals received repeated intraperitoneal administration of cyclosporine A (10 or 20 mg/kg/day for 14 days, n = 5) or vehicle (saline solution, n = 5) as control-2. The dose and period of administration of cyclosporine A were selected based on previous studies [14–16]. Other groups of rats received a single oral administration of 4,4′-methylene dianiline (75 mg/kg, n = 5), α-naphthylisothiocyanate (75 mg/kg, n = 5) or vehicle (0.5% methylcellulose solution, n = 5) as control-3. Under anaesthesia with pentobarbital, the common bile duct was ligated (n = 3). Control animals underwent sham operation (control-4, n = 3).

This study was approved by the Eisai Laboratory Animal Care and Use Committee. All experiments were carried out in accordance with the Guiding Principles for the Care and Use of Laboratory Animals adopted by the Japanese Pharmacological Society, and Eisai's guidelines on animal experimentation (Eisai, Japan). Every effort was made to reduce the number of animals used in the study and to minimize their suffering.

Clinical pathology and histopathology. Blood samples (0.3 ml) were collected from the tail vein prior to administration and 4, 7, and 14 days after administration in the cyclosporine A-treated groups; at 8 hrs and 1, 2, and 4 days after administration in the 4,4′-methylene dianiline- and α-naphthylisothiocyanate-treated groups; and prior to treatment and 2 and 4 days after treatment in the bile duct ligation groups. Serum levels of alkaline phosphatase, alanine aminotransferase, aspartate aminotransferase, γ-glutamyltranspeptidase, total bilirubin, and total bile acids (except in the 4,4′-methylene dianiline/α-naphthylisothiocyanate-treated groups) and biochemical markers of renal function (urea nitrogen and creatinine) were measured with a 7180 automated analyser (Hitachi, Tokyo, Japan) using appropriate kits. Dunnett's tests were used to compare clinical chemical data among groups.

Animals were euthanized by exsanguination under isoflurane anaesthesia and necropsied on the last day. The liver and kidneys were collected and fixed in neutral-buffered 10% formalin and were processed for microscopic examination of routine-paraffin embedded sections stained with haematoxylin and eosin.

Urine collection and ^{1}H nuclear magnetic resonance measurement. Twenty-four-hour urine samples were collected to analyse day-to-day change in urinary metabolites because the treatment (cyclosporine A, 4,4′-methylene dianiline, α-naphthylisothiocyanate and bile duct ligation) employed in this study causes cholestatic injury lasting more than 4 days. Urine samples were collected in a flask containing 1% sodium azide from rats housed in metabolic cages during the following periods: in the 4,4′-methylene dianiline-treated groups (50, 100, and 250 mg/kg), from pre-administration to 3 days after administration; from pre-administration to 14 days after administration in the cyclosporine A-treated groups; pre-administration and 0–4 hr, 4–8 hr, 8–24 hr, 1–2 days, 2–3 days, and 3–4 days after administration in the 4,4′-methylene dianiline (75 mg/kg) and α-naphthylisothiocyanate-treated groups; and from pre-treatment to 4 days after treatment in the bile duct ligation groups. Samples were frozen at −20° until nuclear magnetic resonance spectroscopic analysis.

To minimize pH variation in the urine samples, 300 μl of buffer solution (0.2 M Na_2HPO_4/0.2 M NaH_2PO_4, pH 7.41) was mixed with 600 μl aliquots of urine. One hundred microlitres of 11 mM 3-(trimethylsilyl)propionic-2,2,3,3-d_4 acid sodium salt (as an internal chemical shift reference at 0.00 ppm) in D_2O (for field-frequency lock) was added, and the resulting solution was left to stand for 10 min. Samples were centrifuged at 15,490 ×*g* for 10 min. at 10° to remove any precipitates. The supernatant (650 μl) was placed in a 5 mm glass-tube (Wako Pure Chemical Industries, Osaka, Japan) and analysed at 298 K by ^{1}H nuclear magnetic resonance spectroscopy at 600.13 MHz using a Bruker AVANCE 600 spectrometer (Bruker Biospin, Rheinstetten, Germany). In total, 16 transients were collected into 64 K data points using the 1D-NOESY pulse sequence with solvent presaturation at the water frequency during relaxation delay (5 s) and a mixing time (t_m) of 100 ms. Summed free induction decays were multiplied by an exponential weighting function corresponding to a line broadening of 0.3 Hz before Fourier transformation. Fourier-transformed ^{1}H nuclear magnetic resonance spectra were manually phased, baseline-corrected and referenced to 3-(trimethylsilyl)-propionic 2,2,3,3-d_4 acid sodium salt (0.00 ppm) using TOPSPIN (version 2.0, Bruker).

Data reduction, clustering and pattern detection analysis of ^{1}H nuclear magnetic resonance spectral data and metabolite identification. Each spectrum recorded was reduced to 202 integrated regions of equal

width (0.04 ppm) corresponding to the region 0.42–10.00 ppm using AMIX (version 3.5, Bruker). The area for each segmented region was expressed as an integral value, resulting in an intensity distribution description of the entire spectrum with 202 variables. The region between 6.00 and 4.50 ppm was set to zero integral in order to remove effects of variation in the suppression of water resonance and the effects of variation in the urea signal caused by partial saturation via solvent-exchanging protons. To avoid including parent and metabolised drugs in the analysis, certain regions of the nuclear magnetic resonance spectra were omitted. For 4,4′-methylene dianiline the spectral peaks at 6.82, 6.46, and 3.78 ppm were removed [17], for α-naphthylisothiocyanate the aromatic regions were omitted [8], and for cyclosporine A the spectral peak at 3.70 ppm was removed [18]. All remaining spectral segments were scaled to the total integrated area of the spectrum to reduce variation in concentration. These data were collected into Excel (Microsoft, Excel 2003, SP2) data tables, in which each row included the integral descriptors for an nuclear magnetic resonance spectrum.

The signal pulse and nuclear magnetic resonance spectral data sets were imported into the Spotfire® Decision Site 8.1.1 software package (Tibco Software, CA, USA). For pattern detection, heat-map analysis was performed to characterize and to verify area intensities of these spectral chemical shifts. Chemical shifts considered to be induced by treatment were then clustered by pattern of alteration using K-means clustering analysis, a type of non-hierarchical clustering.

Based on these analyses, candidate metabolites in urine were identified by the NMR suite® (version 5.1, Chenomx, Alberta, Canada) [19], which has a database of about 200 pure compounds to analyse the 1D nuclear magnetic resonance spectra, and can compare the spectral signatures to those found in the urine spectrum and give quantitative metabolic profiles [20–23]. We also referred to data in the literature [24–26] for the assignment of metabolites, ensuring recognition of patterns of change in metabolites over time.

Dunnett's tests were used to compare area intensity of chemical shift data among groups.

Results

Changes in metabolites in 4,4′-methylene dianiline (50, 100, and 250 mg/kg) treatment groups.

Changes in clinical pathological parameters of 4,4′-methylene dianiline-treated groups (50, 100, and 250 mg/kg) are shown in table 1. From the 50 mg/kg (minimum toxic dose) dose group, 4,4′-methylene dianiline treatment elevated serum levels of alanine aminotransferase, aspartate aminotransferase, γ-glutamyltranspeptidase and total bilirubin above values in the control. Urine nuclear magnetic resonance spectra were further examined by heat-map analysis using the Spotfire®, which revealed that the area intensity of proton signals from 0.66 to 1.90 ppm increased in a dose-dependent manner (fig. 1). The endogenous metabolites that were increased in 4,4′-methylene dianiline-treated groups as observed on ^{1}H nuclear magnetic resonance analysis of urine were identified using the NMR suite® and summarized in table 2. Metabolites corresponding to chemical shifts in the region 0.66 to 1.90 ppm included bile acids, branched-chain amino acids (isoleucine, leucine, and valine) and catabolites of branched-chain amino acids. Pattern detection by K-means clustering analysis (fig. 2) revealed that bile acids (fig. 2A), valine (fig. 2B) and methyl malonate (fig. 2C) in urine increased dose-dependently and significantly at doses of 100 and 250 mg/kg after treatment with 4,4′-methylene dianiline. We have also measured the concentration of bile acids in urine samples by LC/MS/MS

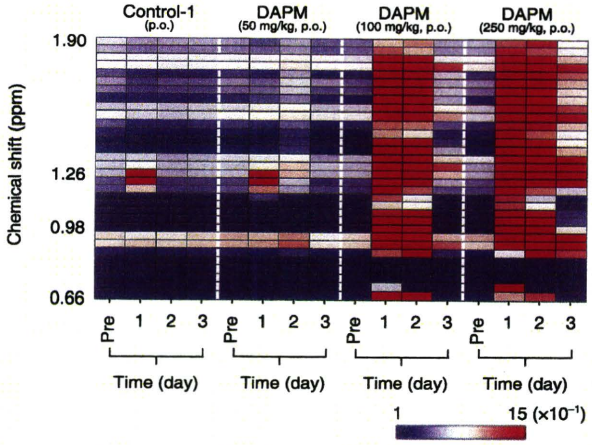

Fig. 1. Clustered heat-map for urinary metabolite nuclear magnetic resonance (NMR) following administration of 4,4′-methylene dianiline (DAPM, 50, 100, and 250 mg/kg, oral administration, n = 5/dose group) and control (Control-1: 0.5% methylcellulose solution, oral administration, n = 5) animals. The colours of the heat map represent the area intensity of chemical shifts from 0.66 to 1.90 ppm: blue for low, white for intermediate and red for high area intensity.

Table 1.

Changes in serum biochemistry parameters of rats given 4,4′-methylene dianiline (DAPM).

	Control-1 p.o., 0.5% methyl cellulose	DAPM p.o., 50 mg/kg		DAPM p.o., 100 mg/kg		DAPM p.o., 250 mg/kg	
Group	Total	1-day	2-day	1-day	2-day	1-day	2-day
ALP (mU/ml)	972 ± 144	946 ± 190	1047 ± 343	2318 ± 1168[1]	2498 ± 852[1]	3593 ± 1491[1]	4086 ± 1456[1]
ALT (mU/ml)	42 ± 5	141 ± 190	350 ± 425[1]	611 ± 289[1]	1894 ± 406[1]	1018 ± 148[1]	1992 ± 764[1]
AST (mU/ml)	112 ± 19	198 ± 170	392 ± 387[1]	933 ± 388[1]	3015 ± 1431[1]	1353 ± 264[1]	3418 ± 1623[1]
GGT (mU/ml)	1 ± 1	1 ± 1	2 ± 1[1]	12 ± 5[1]	15 ± 5[1]	8 ± 2[1]	5 ± 4[1]
Total bilirubin (mg/dl)	0.06 ± 0.02	0.33 ± 0.47[1]	0.29 ± 0.46[1]	3.11 ± 1.70[1]	9.72 ± 5.01[1]	3.79 ± 1.33[1]	11.18 ± 1.80[1]

ALP, alkaline phosphatase; ALT, alanine aminotransferase; AST, aspartate aminotransferase; GGT, γ-glutamyltranspeptidase; p.o., oral administration.

Results are expressed as means ± S.D. of five animals.

[1]Significantly different from control-1 ($P < 0.05$).

Table 2.
The endogenous metabolites increased in the 4,4′-methylene dianiline-treated group observed in the ^{1}H nuclear magnetic resonance analysis of rat urine.

Chemical shift (ppm)	Metabolite[1]
0.66, 0.70, 1.34, 1.38, 1.62, 1.66, 1.74	Bile acid (cholate)
0.90, 1.10	Isoleucine
0.90, 1.58	n-butyrate
0.94, 1.70	Leucine
0.98, 1.02	Valine
1.06	Propionate
1.22	Methyl malonate
1.26	3-Hydroxyisovalerate
1.30	Valerate
1.46	Alanine
7.98, 8.02	Amide NH-signals of conjugated bile acid

[1]Candidate metabolites were identified by the NMR suite® [19], as well as assignments on the basis of data in the literature [24–26].

method in 4,4′-methylene dianiline experiments, and confirmed that there is a dose-dependent increase in concentration of urinary bile acids, and a good correlation between results obtained with nuclear magnetic resonance and LC/MS/MS methods (data not shown).

Clinical pathology.
Changes in clinical pathological parameters in the cyclosporine A-, 4,4′-methylene dianiline-, α-naphthylisothiocyanate- and bile duct ligation-treated groups are presented in table 3. The dose of 4,4′-methylene dianiline 75 mg/kg was selected to induce moderate toxicological changes. In the cyclosporine A-treated group (upper, table 3), decreases in serum levels of alkaline phosphatase, alanine aminotransferase, and aspartate aminotransferase were observed in the 20 mg/kg dose group from 4 days. Serum level of aspartate aminotransferase in the 10 mg/kg dose group decreased from 7 days. Only the 10 mg/kg dose group exhibited a statistically significant increase in γ-glutamyltranspeptidase. In animals treated with cyclosporine A, serum total bilirubin and total bile acid levels increased significantly from 4 days, by about 3–4 times and 10–19 times, respectively. In the 4,4′-methylene dianiline-, α-naphthylisothiocyanate- and bile duct ligation-treated groups (middle and bottom of table 3), serum levels of alkaline phosphatase, alanine aminotransferase, aspartate aminotransferase, γ-glutamyltranspeptidase, and total bilirubin increased significantly, with peaks at 1 or 2 days after treatment, exhibiting the features of cholestasis.

There were no significant changes in renal function parameters in any (cyclosporine A, 4,4′-methylene dianiline, α-naphthylisothiocyanate or bile duct ligation) of the treated groups (data not shown).

Histopathology.
Pathological findings in rats are presented in table 4. No remarkable hepatic histological changes were observed in the control group or the group treated with cyclosporine A

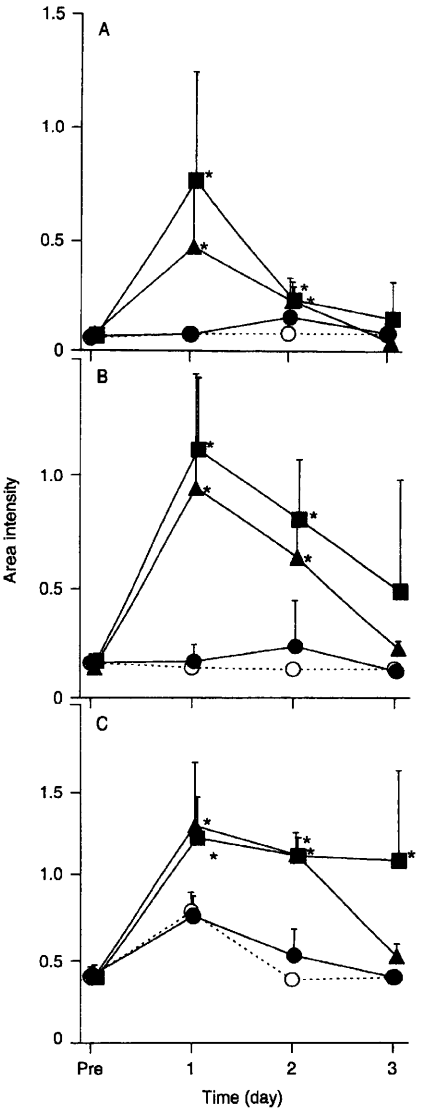

Fig. 2. Change in mean area intensity of chemical shifts for bile acids (A), valine (B) and methyl malonate (C). Animals treated with: vehicle (○: 0.5% methylcellulose solution, oral administration) or 4,4′-methylene dianiline (DAPM, ●: 50 mg/kg, ▲: 100 mg/kg, or ■: 250 mg/kg, oral administration). Each point represents means ± S.D. of five animals. Significant difference from the control group, *$P < 0.05$.

for 14 days. In the 4,4′-methylene dianiline-treated group, hepatic changes characterized by exfoliated necrotic of biliary epithelial cells and necrosis of hepatocyte were observed after 8 hrs, and bile duct hyperplasia, periportal inflammation with oedema and fibrosis were observed after 1 and 4 days. In the α-naphthylisothiocyanate-treated group, hepatic changes characterized by bile duct hyperplasia and fibrosis in the periportal area were observed. In the bile duct ligation-treated group, bile duct changes characterised by bile duct hyperplasia, periportal inflammation, and fibrosis and necrosis of hepatocyte were observed.

Table 3.

Changes in serum biochemistry parameters of rats given cyclosporine A (CyA), 4,4′-methylene dianiline (DAPM), a-naphthylisothiocyanate (ANIT) or bile duct ligation (BDL).

Group	Control-2	CyA (i.p., 10 mg/kg)				CyA (i.p., 20 mg/kg)			
	Total	Pre	4-day	7-day	14-day	Pre	4-day	7-day	14-day
ALP (mU/ml)	1437 ± 350	1536 ± 258	1238 ± 218	1418 ± 322	1264 ± 316	1302 ± 225	997 ± 189[1]	1181 ± 384	859 ± 90[1]
ALT (mU/ml)	42 ± 8	41 ± 3	34 ± 2	33 ± 2	43 ± 4	42 ± 5	32 ± 4[1]	32 ± 4a	34 ± 8
AST (mU/ml)	91 ± 6	104 ± 14	86 ± 11	62 ± 4[1]	67 ± 8[1]	96 ± 12	65 ± 7[1]	62 ± 18[1]	56 ± 6[1]
GGT (mU/ml)	1 ± 1	1 ± 0	0 ± 1	2 ± 0[1]	1 ± 0	1 ± 0	0 ± 0	1 ± 0	1 ± 0
Total bilirubin (mg/dl)	0.05 ± 0.01	0.06 ± 0.00	0.14 ± 0.03[1]	0.16 ± 0.01[1]	0.14 ± 0.01[1]	0.04 ± 0.01	0.15 ± 0.03[1]	0.19 ± 0.03[1]	0.17 ± 0.03[1]
Total bile acid (μmol/l)	6.2 ± 4.4	9.1 ± 6.1	113.0 ± 64.0[1]	97.0 ± 48.7[1]	60.1 ± 60.0[1]	4.1 ± 0.3	66.5 ± 53.4[1]	103.4 ± 42.6[1]	88.4 ± 46.2[1]

Group	Control-3	DAPM (p.o., 75 mg/kg)				ANIT (p.o., 75 mg/kg)			
	Total	8 hrs	1-day	2-day	4-day	8 hrs	1-day	2-day	4-day
ALP (mU/ml)	1508 ± 391	1105 ± 157	3871 ± 770[2]	3343 ± 1206[2]	2033 ± 363[2]	1315 ± 214	1281 ± 142	2361 ± 317[2]	1842 ± 256
ALT (mU/ml)	47 ± 6	57 ± 23	473 ± 169[2]	850 ± 433[2]	68 ± 9	47 ± 6	94 ± 31	1049 ± 386[2]	139 ± 31[2]
AST (mU/ml)	107 ± 20	169 ± 62	770 ± 280[2]	1139 ± 680[2]	81 ± 8	95 ± 10	204 ± 55[2]	2056 ± 995[2]	155 ± 33[2]
GGT (mU/ml)	1 ± 1	3 ± 2[2]	11 ± 3[2]	9 ± 4[2]	1 ± 1	1 ± 0	5 ± 3[2]	6 ± 0[2]	1 ± 0
Total bilirubin (mg/dl)	0.06 ± 0.02	0.22 ± 0.10[2]	2.68 ± 0.38[2]	5.65 ± 2.82[2]	0.51 ± 0.11[2]	0.09 ± 0.04	0.87 ± 0.58[2]	6.73 ± 1.67[2]	1.06 ± 0.38[2]
Total bile acid (μmol/l)	–	169.9[3]	521.8[3]	–	–	–	–	–	–

Group	Control-4	BDL		
	Total	Pre	2-day	4-day
ALP (mU/ml)	573 ± 209	672 ± 126	2948 ± 768[4]	1281 ± 288[4]
ALT (mU/ml)	37 ± 24	32 ± 2	1565 ± 625[4]	445 ± 184[4]
AST (mU/ml)	89 ± 35	119 ± 8	2219 ± 383[4]	970 ± 32[4]
GGT (mU/ml)	1 ± 1	0 ± 0	7 ± 6[4]	11 ± 8[4]
Total bilirubin (mg/dl)	0.07 ± 0.01	0.07 ± 0.01	9.07 ± 3.03[4]	14.76 ± 10.14[4]
Total bile acid (μmol/l)	13.1 ± 7.4	7.2 ± 4.8	198.4 ± 164.0[4]	153.5 ± 13.2[4]

ALP, alkaline phosphatase; ALT, alanine aminotransferase; AST, aspartate aminotransferase; GGT, γ-glutamyltranspeptidase; Control-2, intraperitoneal administration (i.p.), saline solution; Control-3, oral administration (p.o.), 0.5% methyl cellulose; Control-4, sham operation; –, Not measured. Results are expressed as means ± S.D. of five (CyA, ANIT, and DAPM groups) or three (BDL groups) animals.

[1]Significantly different from Control-2 ($P < 0.05$).

[2]Significantly different from Control-3 ($P < 0.05$).

[3]Means of two animals.

[4]Significantly different from Control-4 ($P < 0.05$).

Table 4.

Pathological findings of rats given cyclosporine A (CyA), 4,4′-methylene dianiline (DAPM), a-naphthylisothiocyanate (ANIT) or bile duct ligation (BDL).

		CyA				DAPM			ANIT	BDL
		10 mg/kg		20 mg/kg		75 mg/kg			75 mg/kg	
Organ	Pathological findings	7 day	14 day	7 day	14 day	8hr	1 day	4 day	4 day	4 day
Liver	Necrosis, biliary epithelial cell	–	–	–	–	1+	1+	–	–	–
	Periportal inflammation	–	–	–	–	–	1+	1+	–	1+
	Periportal fibrosis	–	–	–	–	–	–	2+	1+	1+
	Hyperplasia, bile duct	–	–	–	–	–	1+	1+	1+	2+
	Necrosis, hepatocyte	–	–	–	–	1+	1+	1+	–	1+
Kidney	Tubular degeneration	1+	1+	2+	3+	–	–	–	–	–

Grade: –, No histopathological changes; 1+, slight; 2+, moderate; 3+, marked.

In the cyclosporine A-treated group, histological changes characterised by tubular degeneration of kidney were noted. There were no renal pathological changes in the 4,4′-methylene dianiline-, α-naphthylisothiocyanate- or bile duct ligation-treated groups.

^{1}H nuclear magnetic resonance spectral analysis of urine samples.

Changes in peaks in the cyclosporine A-, 4,4′-methylene dianiline-, α-naphthylisothiocyanate- and bile duct ligation-treated groups were evaluated by heat-map clustering (fig. 3). In the cyclosporine A-treated groups, area intensities of the region 0.66 to 1.90 ppm were suppressed from 6 days (20 mg/kg) or 7 days (10 mg/kg) of administration to the end of the 14-day treatment period, but were enhanced after treatment with 4,4′-methylene dianiline (75 mg/kg), α-naphthylisothiocyanate and bile duct ligation.

Chemical shifts of peaks induced by treatment with cyclosporine A, 4,4′-methylene dianiline, α-naphthylisothiocyanate or bile duct ligation were clustered by pattern of alteration, as determined by K-means clustering analysis. Seven characteristic clusters of changes were found among all treated

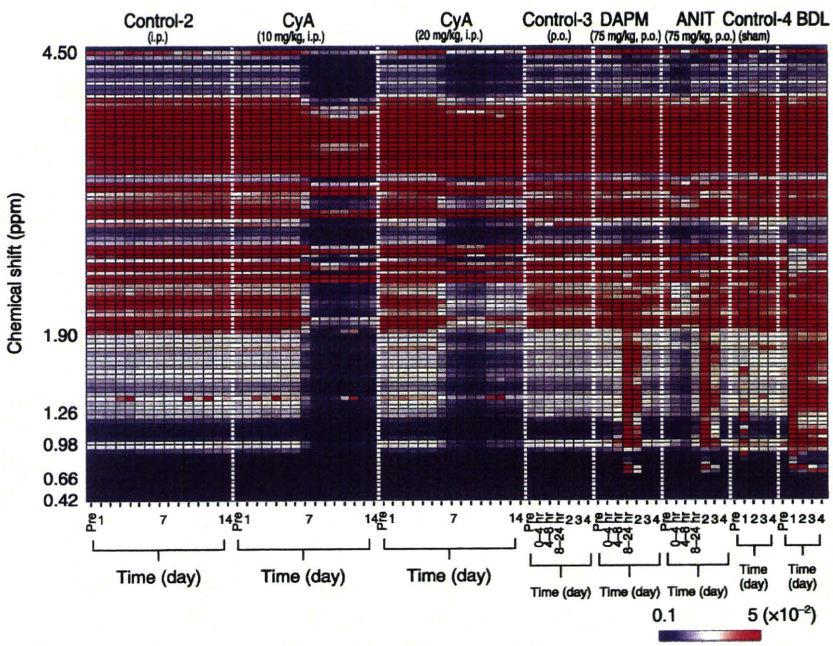

Fig. 3. Clustered heat-map for urinary metabolite nuclear magnetic resonance (NMR) following administration of cyclosporine A (CyA, 10 and 20 mg/kg, intraperitoneal administration, n = 5), 4,4′-methylene dianiline (DAPM, 75 mg/kg, oral administration, n = 5), α-naphthylisothiocyanate (ANIT, 75 mg/kg, oral administration, n = 5) or bile duct ligation (BDL, n = 3) and control (Control-2: saline solution, intraperitoneal administration, n = 5; Control-3: 0.5% methyl cellulose, oral administration, n = 5; Control-4: sham operation, n = 3) animals. The colours of the heat map represent the area intensity of chemical shifts from 0.42 to 4.50 ppm: blue for low, white for intermediate and red for high area intensity.

Table 5.

The endogenous metabolites of rat urine induced by treatment with cyclosporine A, 4,4′-methylene dianiline, a-naphthylisothiocyanate or bile duct ligation were clustered by pattern of alteration using K-means clustering analysis.

Cluster	Chemical shift (ppm)	Metabolite[1]
Cluster 1	2.42	Succinate
	2.46, 3.02	2-Oxyglutarate
	2.50, 2.54, 2.66	Citrate
	2.70	Sarcosine
	6.54	Fumarate
	3.98, 7.54, 7.58, 7.62, 7.66, 7.82, 7.86	Hippurate
Cluster 2	7.10	Histidine
	7.18	Tyrosine
	7.22, 7.30, 7.34	Tryptophan
	7.26	3-Indoxyl sulphate
	7.38, 7.42	Phenylalanine
Cluster 3	2.06, 3.34, 4.14	Proline
	2.26, 3.66	Acetoacetate
	2.86	*N,N*-dimethylglycine
	4.02, 4.50	Ascorbate
	4.06	Creatinine
	4.26	Threonine
	4.30, 6.10	Adenosine
	6.86, 7.70	4-aminohippurate
	8.46	Formate
Cluster 4	3.22, 3.38, 3.46, 3.50, 3.54, 3.74, 3.82, 3.86	Glucose
	3.26	Trimethylamine-*N*-oxide
	3.42	Taurine
	3.90	Betaine
Cluster 5	0.66, 0.70, 1.34, 1.38, 1.62, 1.66, 1.74	Bile acid (cholate)
	0.90, 1.10	Isoleucine
	0.90, 1.58	n-butyrate
	0.94, 1.70	Leucine
	0.98, 1.02	Valine
	1.06	Propionate
	1.22	Methyl malonate
	1.26	3-hydroxyisovalerate
	1.30	Valerate
	1.46	Alanine
	7.98, 8.02	Amide NH-signals of conjugated bile acid
Cluster 6	1.78, 1.82, 1.86, 3.10	Ornithine
	1.90	Acetate
	1.98, 2.10, 2.14, 2.18, 2.34, 2.38	Homoserine
Cluster 7	8.90, 8.98, 9.26	*N*-methylnicotinamide

[1]Candidate metabolites were identified by the NMR suite® [19], as well as assignments on the basis of data in the literature [24–26].

groups and candidate metabolites were identified (table 5). Changes in mean area intensity of chemical shifts about clusters are shown in figs 4 and 5. The first cluster, including sarcosine, represented the area intensity of chemical shifts unchanged from 1 to 6 days of administration and suppressed thereafter in the cyclosporine A-treated groups (fig. 4A), as well as those suppressed by treatment with 4,4′-methylene dianiline, α-naphthylisothiocyanate or bile duct ligation (fig. 4B). The second one, which included histidine, represented the area intensity of chemical shifts unchanged after cyclosporine A treatment (fig. 4C) and those transiently enhanced and peaking at 24-hr post-administration in the 4,4′-methylene dianiline-treated group (fig. 4D). The third one, which included acetoacetate, represented the area intensity of chemical shifts enhanced from 1 to 6 days of administration in the cyclosporine A-treated group (fig. 4E) and those enhanced by treatment with 4,4′-methylene dianiline and α-naphthylisothiocyanate, but unchanged in the bile duct ligation-treated group (fig. 4F). The fourth one, which included glucose, represented the area intensity of chemical shifts increased in the cyclosporine A-treated groups (fig. 4G) and transiently increased in the α-naphthylisothiocyanate-treated group (fig. 4H).

The fifth cluster included bile acids, valine and methyl malonate (fig. 5). Other metabolites belonging to this cluster are shown in table 2 and were identified as n-butyrate, propionate, 3-hydroxyisovalerate, valerate, leucine, isoleucine, alanine, and amide NH-signals of conjugated bile acids. Changes in area intensities for bile acids, valine and methyl malonate are plotted separately. In the case of bile acids,

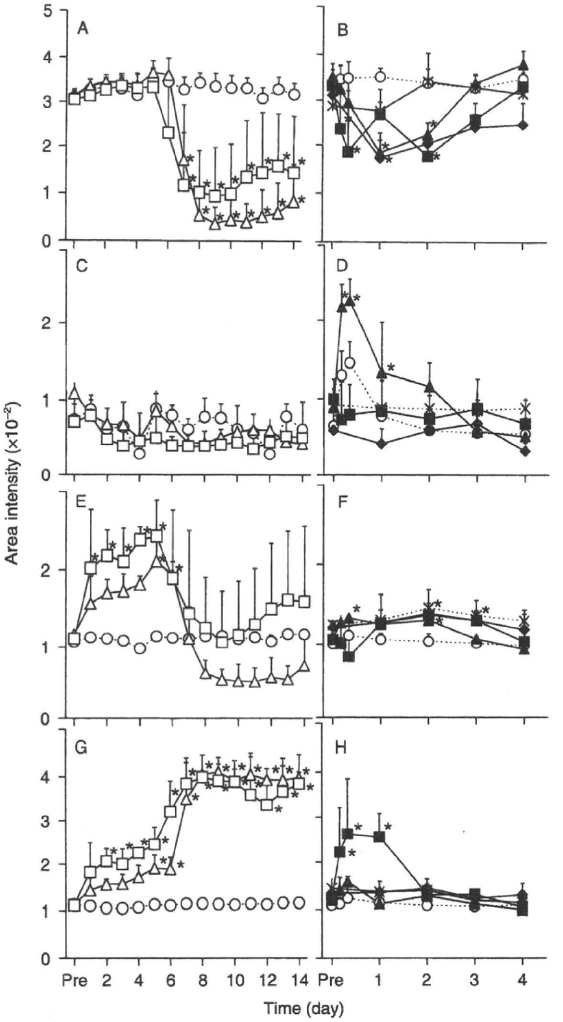

Fig. 4. Change in mean area intensity of chemical shifts for sarcosine (A, B), histidine (C, D), acetoacetate (E, F) and glucose (G, H). Animals treated with: vehicle (○) or cyclosporine A (CyA, △: 10 mg/kg and □: 20 mg/kg, intraperitoneal administration, n = 5) are visualized in A, C, E, and G; vehicle (○), sham operation (×), 4,4′-methylene dianiline (DAPM, ▲: 75 mg/kg, oral administration, n = 5), α-naphthylisothiocyanate (ANIT, ■: 75 mg/kg, oral administration, n = 5), and bile duct ligation (BDL, ◆: n = 3) are visualized in B, D, F, and H. Each point represents means ± S.D. of three or five animals. Significant difference from the control group, *P < 0.05.

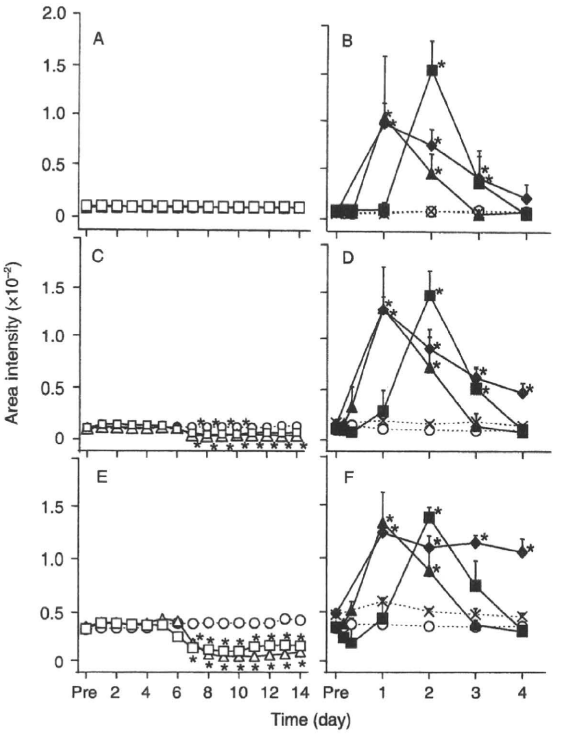

Fig. 5. Change in mean area intensity of chemical shifts for bile acids (A, B), valine (C, D) and methyl malonate (E, F). Animals treated with: vehicle (○) or cyclosporine A (CyA, △: 10 mg/kg and □: 20 mg/kg, intraperitoneal administration, n = 5) are visualized in A, C, and E; vehicle (○), sham operation (×), 4,4′-methylene dianiline (DAPM, ▲: 75 mg/kg, oral administration, n = 5), α-naphthylisothiocyanate (ANIT, ■: 75 mg/kg, oral administration, n = 5), and bile duct ligation (BDL, ◆: n = 3) are visualized in B, D, and F. Each point represents means ± S.D. of three or five animals. Significant difference from the control group, *P < 0.05.

cyclosporine A treatment (fig. 5A) did not affect area intensities, but 4,4′-methylene dianiline, α-naphthylisothiocyanate, and bile duct ligation (fig. 5B) increased it significantly. For valine and methyl malonate, cyclosporine A treatment (fig. 5C and E) decreased area intensities significantly from 7 days compared with control, while 4,4′-methylene dianiline, α-naphthylisothiocyanate and bile duct ligation treatment (figs. 5D and F) increased them.

The sixth cluster, which included acetate, represented the area intensity of chemical shifts unchanged from 1 to 6 days of administration and suppressed thereafter in the cyclosporine A-treated groups, and those enhanced in 4,4′methylene dianiline-, α-naphthylisothiocyanate-, bile duct ligation- and sham operation-treated groups (fig. not shown). The seventh cluster, which included *N*-methylnicotinamide, represented the area intensity of chemical shifts unchanged after treatment of all groups (figure not shown).

Discussion

Hepatotoxicity is the most common complication in drug development, and extensive efforts have been made to minimise the attrition of new drug candidates due to it. Although clinical pathological and histopathological analyses are commonly performed to evaluate hepatotoxicity, new-omics technologies have come to be used increasingly for this purpose.

The purpose of the present study was to determine whether ^{1}H nuclear magnetic resonance-based metabonomics using rat urine samples can discriminate differences in

